



**HAL**  
open science

## Species variation in the hydrogen isotope composition of leaf cellulose is mostly driven by isotopic variation in leaf sucrose

Meisha Holloway-Phillips, Jochem Baan, Daniel Nelson, Marco Lehmann, Guillaume Tcherkez, Ansgar Kahmen

### ► To cite this version:

Meisha Holloway-Phillips, Jochem Baan, Daniel Nelson, Marco Lehmann, Guillaume Tcherkez, et al.. Species variation in the hydrogen isotope composition of leaf cellulose is mostly driven by isotopic variation in leaf sucrose. *Plant, Cell and Environment*, 2022, pp.1-16. 10.1111/pce.14362 . hal-03726246

**HAL Id: hal-03726246**

**<https://hal.inrae.fr/hal-03726246>**

Submitted on 18 Jul 2022

**HAL** is a multi-disciplinary open access archive for the deposit and dissemination of scientific research documents, whether they are published or not. The documents may come from teaching and research institutions in France or abroad, or from public or private research centers.

L'archive ouverte pluridisciplinaire **HAL**, est destinée au dépôt et à la diffusion de documents scientifiques de niveau recherche, publiés ou non, émanant des établissements d'enseignement et de recherche français ou étrangers, des laboratoires publics ou privés.



Distributed under a Creative Commons Attribution - NonCommercial - NoDerivatives 4.0 International License

# Species variation in the hydrogen isotope composition of leaf cellulose is mostly driven by isotopic variation in leaf sucrose

Meisha Holloway-Phillips<sup>1</sup>  | Jochem Baan<sup>1</sup>  | Daniel B. Nelson<sup>1</sup>  |  
 Marco M. Lehmann<sup>2</sup>  | Guillaume Tcherkez<sup>3,4</sup>  | Ansgar Kahmen<sup>1</sup> 

<sup>1</sup>Department of Environmental Science—Botany, University of Basel, Basel, Switzerland

<sup>2</sup>Research Unit of Forest Dynamics, Research Group of Ecosystem Ecology, Stable Isotope Research Centre, Swiss Federal Institute for Forest, Snow and Landscape Research WSL, Birmensdorf, Switzerland

<sup>3</sup>Research School of Biology, College of Science, Australian National University, Canberra, Australian Capital Territory, Australia

<sup>4</sup>Institut de Recherche en Horticulture et Semences, Université d'Angers, INRAE, Beaucouzé, France

## Correspondence

Meisha Holloway-Phillips, Department of Environmental Science—Botany, University of Basel, Schönbeinstrasse 6, 4056 Basel, Switzerland.

Email: [m.holloway-phillips@unibas.ch](mailto:m.holloway-phillips@unibas.ch)

## Funding information

European Research Council Consolidator Grant, Grant/Award Number: 724750 HYDROCARB; SNSF Ambizione project, Grant/Award Number: 179978 TreeCarbo; Region Pays de la Loire Connect Talent Grant Isoseed, Grant/Award Number: Isoseed

## Abstract

Experimental approaches to isolate drivers of variation in the carbon-bound hydrogen isotope composition ( $\delta^2\text{H}$ ) of plant cellulose are rare and current models are limited in their application. This is in part due to a lack in understanding of how  $^2\text{H}$ -fractionations in carbohydrates differ between species. We analysed, for the first time, the  $\delta^2\text{H}$  of leaf sucrose along with the  $\delta^2\text{H}$  and  $\delta^{18}\text{O}$  of leaf cellulose and leaf and xylem water across seven herbaceous species and a starchless mutant of tobacco. The  $\delta^2\text{H}$  of sucrose explained 66% of the  $\delta^2\text{H}$  variation in cellulose ( $R^2 = 0.66$ ), which was associated with species differences in the  $^2\text{H}$  enrichment of sucrose above leaf water ( $\epsilon_{\text{sucrose}}$ :  $-126\%$  to  $-192\%$ ) rather than by variation in leaf water  $\delta^2\text{H}$  itself.  $\epsilon_{\text{sucrose}}$  was positively related to dark respiration ( $R^2 = 0.27$ ), and isotopic exchange of hydrogen in sugars was positively related to the turnover time of carbohydrates ( $R^2 = 0.38$ ), but only when  $\epsilon_{\text{sucrose}}$  was fixed to the literature accepted value of  $-171\%$ . No relation was found between isotopic exchange of hydrogen and oxygen, suggesting large differences in the processes shaping post-photosynthetic fractionation between elements. Our results strongly advocate that for robust applications of the leaf cellulose hydrogen isotope model, parameterization utilizing  $\delta^2\text{H}$  of sugars is needed.

## 1 | INTRODUCTION

Interest in the oxygen (O) and carbon-bound hydrogen (H) stable isotope composition ( $\delta$ ) of plant cellulose is motivated by the hydrological, physiological and metabolic controls that drive isotopic variation and thus their use as proxies to investigate climate change and plant responses over time. To date, most of the research has focussed on the strength of the environmental (e.g., An et al., 2014; Libby et al., 1976) and physiological signals (e.g., Barbour et al.,

2000b; Scheidegger et al., 2000), essentially assuming that the metabolic component is invariant. However, as more comparisons have been made between plant species, tissues, and contexts, the idea that the plant faithfully records and integrates environmental information has been challenged (e.g., Cheesman & Cernusak, 2016; Waterhouse et al., 2002). Indeed for carbon-bound hydrogen, it is generally accepted that metabolism should influence biosynthetic isotope fractionation (e.g., Augusti et al., 2008; Hayes, 2018; Schmidt et al., 2003), but there have been few attempts to assess how

This is an open access article under the terms of the Creative Commons Attribution-NonCommercial-NoDerivs License, which permits use and distribution in any medium, provided the original work is properly cited, the use is non-commercial and no modifications or adaptations are made.

© 2022 The Authors. *Plant, Cell & Environment* published by John Wiley & Sons Ltd.

significant this effect may be (Augusti et al., 2006; Cormier et al., 2018; Ehlers et al., 2015; Schleucher et al., 1999; Wieloch et al., 2022a, 2022b).

To disentangle the different sources of isotopic variation, semi-mechanistic cellulose isotope models have been developed. The cellulose oxygen isotope model developed by Barbour and Farquhar (2000), is a two-component model which separates source and sink cell processes, where sugars exported from the photosynthesizing 'source' leaf are translocated to the developing 'sink' tissue for cellulose synthesis. The importance of compartmentalizing these two processes is reflected in the different isotopic compositions of their water pools—leaf water generally being evaporatively  $^{18}\text{O}$  and  $^2\text{H}$  enriched above sink cell water, which, in turn, is usually assumed to reflect the isotopic composition of source water. Furthermore, the reactions involving isotopic exchange of oxygen during hydration of carbonyl groups occur in both source and sink cell metabolism. As such, the leaf water evaporative signal imprinted on exported sugars becomes 'damped' during isotopic exchange with sink cell water, and therefore, the correlation between cellulose  $\delta^{18}\text{O}$  and leaf water falls below the expected regression line.

DeNiro and Cooper (1989) suggested that the key metabolic steps involved in oxygen isotopic exchange occur during the cycling of hexose monophosphates to triose phosphates where there are three main enzyme reactions that result in hydrolysis or indirect exchange with water through tautomerisation and the formation of isomers leading to a rearrangement of sugar phosphates. These include (1) interconversion between fructose 6-phosphate to fructose 1,6-bisphosphate (F-1,6-BP) by pyrophosphate: fructose-6-phosphate 1-phosphotransferase (PF6P); (2) hydrolysis of F-1,6-BP to dihydroxyacetone (DHAP) and glyceraldehyde-3-phosphate (GAP) by aldolase; and (3) the interconversion of DHAP and GAP by triosephosphate isomerase (TPI) (Augusti et al., 2006; Farquhar et al., 1998). Evidence for this rapid cycle, is limited to the study by Hill et al. (1995) in tree rings. It is generally assumed that oxygen isotope exchange occurs at equilibrium with an  $^{18}\text{O}$  enrichment of around 27‰ of the carbonyl oxygen relative to water (Sternberg & DeNiro, 1983). Experimental validation of this assumption comes from oxygen isotope measurements of exported sugar (Cernusak et al., 2003); although temperature can modify this value (Sternberg & Ellsworth, 2011). Complications in interpreting the measured isotopic offset between sugars and water can occur if assimilation rate and hence sugar synthesis does not occur across the entire leaf as assumed in sampling the bulk leaf water isotope composition (Lehmann et al., 2017), because the isotope composition of leaf water, and hence sugar, varies spatially (Cernusak et al., 2016).

Barbour and Farquhar (2000) postulated that one important factor linking triose-hexose futile cycling to the extent of oxygen isotope exchange is how quickly sucrose is used for cellulose synthesis, whereby a longer residence time of sugars in sink cells increases the opportunity for hexose phosphates to cycle through triose phosphates and thereby undergo isotopic exchange. Song et al. (2014) followed up on this hypothesis, relating isotopic exchange derived from the mechanistic model to the turnover time of nonstructural carbohydrates available for

cellulose synthesis. Growing *Ricinus communis* (castor bean) under two different light intensities and relative humidities, they were able to manipulate both the extent to which oxygen isotopically exchanged with sink cell water and the turnover time of sugars, and provided strong evidence that the two processes are positively related. Emerging patterns of isotopic exchange across environmental gradients (Cheesman & Cernusak, 2016) and phenological stage (e.g., Gessler et al., 2009; Nabeshima et al., 2018; Szejner et al., 2020), suggests that the mechanistic model could be used as a tool to explore the physiological significance of triose-hexose phosphate cycling, which remains little understood (Amthor et al., 2019).

The original cellulose hydrogen isotope model for carbon-bound hydrogen was developed by Yakir and DeNiro (1990) and shares both similarities and differences with the oxygen model. Instead of separating source and sink cell processes, division was made between photosynthetic and post-photosynthetic reactions; the latter being downstream from triose-phosphate export from the chloroplast. As such, the post-photosynthetic reactions occur in both leaf water and sink cell water. Parameterization of the model was conducted in the aquatic plant, *Lemna gibba* L., and required growing plants under autotrophic and heterotrophic (fed with sucrose of a known isotope composition) conditions under 100% humidity to prevent isotopic gradients from source to leaf water. However, in the application to terrestrial plants, Roden et al. (2000) assigned the post-photosynthetic processes to the sink cell only, in line with the conceptual model for oxygen and assumed the isotope fractionation values derived by Yakir and DeNiro (1990) were still valid.

Biochemical  $^2\text{H}$  isotope fractionation associated with photosynthesis was estimated to be  $-171\text{‰}$  (isotopic offset between triose-phosphates exported from the chloroplast and leaf water) (Yakir & DeNiro, 1990). This dramatic  $^2\text{H}$ -depletion was assumed to reflect the  $^2\text{H}$ -depleted free proton pool available for  $\text{NADP}^+$  reduction, due to the equilibrium isotope fractionation between hydrogen ions and water (Luo et al., 1991) and isotope fractionations during protonation by  $\text{NADPH}$  and subsequent transfer during the reduction of glyceraldehyde-3-phosphate (GAP). In comparison, the biochemical isotope fractionation associated with post-photosynthetic reactions was found to be of similar magnitude but positive, with a net effect of  $+158\text{‰}$ . The key biochemical reactions associated with  $^2\text{H}$ -enrichment were suggested to be the same reactions that are associated with oxygen isotope exchange during triose-hexose phosphate interconversions (Augusti et al., 2006; Yakir & DeNiro, 1990). However, the mechanisms for oxygen and carbon-bound hydrogen isotope exchange are quite different, with hydrogen isotope exchange always requiring enzymes for the cleavage and protonation of compounds during chemical reactions, whereas oxygen isotope exchange can occur via hydration of the carbonyl group via acid-base catalysis with water alone. For example, TPI can mediate hydrogen isotope exchange with bulk water during proton shift from C-3 pro-R position of DHAP to C-2 of GAP (Knowles & Albery, 1977; Rieder & Rose, 1959), whereas oxygen isotope exchange from the diol intermediate is unlikely; however, both trioses themselves will be subject to oxygen isotope exchange in their

carbonyl groups (Byrn & Calvin, 1966), that is, oxygen isotope exchange is not enzyme-catalysed by TPI and can happen independently.

Enzyme-mediated isotope exchange of carbon-bound hydrogen tends to have large kinetic isotope effects owing to the large mass difference between protium and deuterium. Continuing the example above, the primary kinetic isotope effect (KIE) associated with TPI is 2.9 ( $k_H/k_D$ ; in the direction DHAP to GAP) (Leadlay et al., 1976), compared with equilibrium isotope exchange of carbonyl-oxygen, which is estimated to be 1.028 (Sternberg & DeNiro, 1983). Furthermore, whilst there is indirect evidence for a temperature dependent offset between carbonyl-oxygen and water (Hirl et al., 2021; Sternberg & Ellsworth, 2011), in general, there has been little evidence that disequilibrium is commonly observed (Barbour, 1999; Lehmann et al., 2017). On the contrary, in bidirectional reactions, the observed hydrogen isotope effect will be dependent on the flux through the forward and backward reactions, which have independent kinetic isotope effects. As such, the net isotope fractionation associated with all post-photosynthetic reactions is likely to be variable and not fixed, as is commonly interpreted from the Yakir and DeNiro (1990) experiment. For detailed descriptions on the bonds involved in key reactions we refer the reader to Tcherkez (2010). For the individual elements we suggest for oxygen isotope effects in plants: Farquhar et al. (1998), Schmidt et al. (2001), Lehmann et al. (2017) and Ma et al. (2020), and for carbon-bound hydrogen isotope effects in plants: Schmidt et al. (2003), Augusti et al. (2006), Cormier et al. (2018) and Zhou et al. (2018).

The influence of metabolism on net isotope fractionation is the basis of the hydrogen 'metabolic proxy' concept proposed by Augusti et al. (2008) and advanced by Cormier et al. (2018). As to the probability of isotopic exchange occurring, it is still likely to depend on the degree to which sugars cycle via these reactions. Due to the different mechanisms of isotopic exchange between oxygen and carbon-bound hydrogen, it is not obvious that the probability of exchange should be the same; but, early estimates suggest the probability may be proportional (Luo & Sternberg, 1992).

Because the Yakir and DeNiro (1990) experimental approach is difficult to implement in terrestrial plants, validation of biosynthetic hydrogen isotope fractionation factors has been mainly achieved through tuning the model term that describes the fraction of carbon-bound hydrogen that undergoes isotopic exchange during post-photosynthetic reactions (Equation 6), in order for the model to fit the observed  $\delta^2\text{H}$  of cellulose (Roden et al., 2000; Waterhouse et al., 2002). However, to improve the application of cellulose isotope models, independent quantification of all model parameters is required. In this study, we take steps towards achieving this goal by quantifying biosynthetic fractionation during the production of sucrose ( $\epsilon_{\text{sucrose}}$ ; Equation 4) in mature leaves and assessing how  $\epsilon_{\text{sucrose}}$  varies between plant species grown under controlled conditions. Measurements of the  $\delta^2\text{H}$  of leaf sucrose were related to the  $\delta^2\text{H}$  of bulk leaf water, as compared to the isotopic composition of evaporative sites (Roden et al., 2000), on the proviso that isotopic exchange occurs within the cytosol, as is assumed the case for oxygen (Barbour & Farquhar, 2000). When combined with measures of

xylem water and leaf cellulose, we utilize the cellulose isotope model to improve the estimation of the fraction of isotopic exchange that occurs during sink cell metabolism. Further, we test whether the fraction of isotopic exchange is proportional between oxygen and hydrogen and whether sugar turnover time is a good metabolic proxy for understanding variability in isotopic exchange in either element. Finally, we provide a more complete experimental approach that can quantify all parameters in the cellulose hydrogen isotope model along with alternative descriptions of the model that consider complexities in spatial and temporal use of carbon sources and synthesis of leaf cellulose.

## 2 | MATERIALS AND METHODS

### 2.1 | Growth conditions

Plants were grown from seeds in October 2019 in pots of 12 cm diameter and 13.5 cm height, in potting mix fertilized weekly with Hoagland's solution. To have sufficient leaf material of a similar age, two plants were propagated in some pots, including *Gossypium herbaceum* (cotton), *Phaseolus vulgaris* L. var. *vulgaris* cv. 'Neckarkönigin' (bean), *Raphanus sativus* cv. 'Marabelle' (radish), *Lycopersicon esculentum* cv. 'cheery red' (tomato), while only one plant was propagated per pot for *Helianthus herbaceum* cv. 'Waooh' (sunflower), *Cajanus cajan* cv. 'BRG-1' (pigeonpea), and *Nicotiana sylvestris* wild-type (tobacco WT) and phosphoglucosyltransferase mutant (tobacco *pgm*; Hanson & McHale, 1988). There were three pots per species ( $n=3$ ). Pots were randomized and moved every few days on one bench in a glasshouse with average night time temperatures of  $16.7^\circ\text{C} \pm 1.6$  SD, reaching average daytime conditions between 6:00–18:00 of  $24.6^\circ\text{C} \pm 3.8$  SD. Relative humidity was on average  $49.9\% \pm 4.1$  SD during the night and  $43.5\% \pm 4.7$  SD during the day (see Supporting Information: Figure S5.3 for diurnal environmental conditions). Supplemental light was provided for 14 h during the day (6:00–18:00). The light level in the glasshouse was measured using a handheld spectrometer (LI-180; LiCor Inc.). Based on measurements on an overcast day (experiment was conducted in the fall), the lights provided on average  $350 \mu\text{mol m}^{-2} \text{s}^{-1}$  of photosynthetic photon flux density, 20% of which was blue light and with a red to far-red ratio of 1.9. On the days of gas exchange, the light level, based on readings from the LI-6800 internal chamber sensor, was on average  $231.9 \mu\text{mol m}^{-2} \text{s}^{-1} \pm 30.9$  SD at the height of the measured leaves. Plants were watered daily to ensure that the potting mix did not dry out and to reduce the changes in source water isotopic composition associated with soil evaporation.

### 2.2 | Gas exchange

Assimilation rate was measured with a LI-6800 open gas-exchange system (LiCor Inc.) twice—1 day before harvest, and on the day of harvest immediately before the plant was sampled. The results were averaged (see Supporting Information: Table S5.3 for means and

standard deviation of gas exchange parameters). One mature leaf from each pot was measured between 10:00 and 14:00 (total of three measurements per species). A clear-top chamber was used to ensure that the light intensity at plant level was captured. Otherwise the chamber conditions were set to a sample CO<sub>2</sub> concentration of 400 μmol mol<sup>-1</sup>, relative humidity of 45%, 26°C chamber air, a flow of 400 μmol s<sup>-1</sup>, and a chamber over pressure of 0.2 kPa. As these were instantaneous measurements, a measure was taken as soon as the values stabilized (visually) and no leaf was in the chamber beyond 5 min. The instrument was periodically zeroed.

### 2.3 | Sample collection

Plants were destructively harvested ~9 weeks after they were sown. Each species had slightly different sampling requirements due to the size and distribution of leaves. In general, where leaves/leaflets were large enough, leaves were split in half along the mid-vein (the mid-vein always removed) and used for two different analyses (leaf water analysis and sucrose isotope analysis). Specific leaf area (SLA) was measured with a leaf corer of known diameter (10 mm). Three to four disks were taken along the length of the leaf and dried at 55°C before being weighed. SLA was then calculated as  $\pi r^2 \times \text{no. of disks} / \text{total weight (m}^2\text{g}^{-1})$ . Destructive sampling was conducted immediately after each gas exchange measurement on the sampling day.

Leaf and xylem water samples were collected in Exetainer® vials (Labco, Ltd.) and placed on ice before being stored in a -20°C freezer. For the xylem water, the main root collar of each plant was sampled and any soil brushed off before placing in the exetainer (Barnard et al., 2006). Water from roots and leaves were cryogenically extracted on a vacuum distillation system with an open vacuum design, and oxygen and hydrogen isotope compositions were analysed, all according to the protocol of Newberry et al. (2017). Precision of δ<sup>18</sup>O and δ<sup>2</sup>H water measurements for the experimental period were 0.11‰ (n = 163) and 0.3‰ (n = 138), respectively.

Multiple leaves (always fully-expanded and of similar age) were generally collected to make up the sample dry-weight requirements. The same material used to analyse the nonstructural carbohydrates was also used for δ<sup>2</sup>H sugar analyses. This material was immediately microwaved for two cycles of 1 min, dried for 48 h at 55°C, and ground to homogenize the material (Landhäusser et al., 2018). Nonstructural carbohydrates (sucrose, glucose and fructose; NSC) were analysed using the protocol of Landhäusser et al. (2018). The turnover time was calculated according to Song et al. (2014), as NSC content in equivalent mol C m<sup>-2</sup> s<sup>-1</sup> divided by assimilation rate (mol m<sup>-2</sup> s<sup>-1</sup>), and reported in minutes. To convert NSC content to an area basis, SLA was used (see Supporting Information: Table S5.3 for mean and standard deviation of SLA). Leaf material for cellulose extractions was dried at 55°C in a fan-forced oven for two days and combined with the dried material remaining after cryogenic extraction of the leaf water. All material was ground to homogenize before cellulose extraction.

### 2.4 | Cellulose δ<sup>2</sup>H and δ<sup>18</sup>O analyses

Cellulose was extracted based on the Jayme-Wise method, with treatment of the holocellulose using 17% sodium hydroxide to retrieve α-cellulose (Gaudinski et al., 2005). Briefly, approximately, 250 mg of ground, dry leaf material was sealed into filter bags (Ankom; SKU:F57). Lipids were first removed by heating 2:1 mixture of toluene/ethanol in a Soxhlet apparatus for 24 h, followed by another 24 h of ethanol. After drying off solvents, samples were bleached with 1.4% (w/v) sodium chlorite and acetic acid solutions (pH 4-5) in an ultrasonic bath at 70°C. The concentration of the solution was sequentially increased by 1.4% sodium chlorite, and acetic acid added to maintain pH at 4-5, after 3 h and 6 h. Then, after 9 h, samples were bleached once more in a new 4% (w/v) sodium chlorite and acetic acid solution (pH 4-5) for 12 h at 70°C in an ultrasonic bath. Lastly, holocellulose was removed from the samples with a 17% sodium hydroxide solution at room temperature in an ultrasonic bath for 1 h, to obtain α-cellulose. Sodium hydroxide was neutralized by multiple rinses with deionized water in an ultrasonic bath at room temperature, before samples were dried for 48 h at 50°C, milled and approximately 0.5 mg of material weighed into silver cups for isotope analyses.

Cellulose δ<sup>18</sup>O values were determined using a Flash IRMS operated in pyrolysis mode using a glassy carbon reactor configuration operated at 1400°C coupled to a Delta V isotope ratio mass spectrometer (IRMS) through a ConFlo IV Plus interface (Thermo Fisher Scientific). Encapsulated samples were sealed in a Costech Zero-Blank Autosampler (NC Technologies Srl) that was operated at room temperature, and the isolation valve was opened at least 3 h before beginning each analytical run to allow the autosampler and glassy carbon reactor to equilibrate under constant helium carrier gas flow at 100 ml/min. δ<sup>18</sup>O values were normalized to the VSMOW-SLAP scale and are reported in standard delta notation (Vienna Standard Mean Ocean Water; 0‰, and Standard Light Antarctic Precipitation; δ<sup>2</sup>H = -427.5‰, δ<sup>18</sup>O = -55.5‰). Scale normalization was conducted using calibrated in-house organic acid standards, dimethyl benzoic acid, and benzoic acid with known δ<sup>18</sup>O values of +2.89‰ and +23.96‰, respectively. Analytical precision was monitored through repeat analysis of a trimethyl benzoic acid quality control sample with a δ<sup>18</sup>O value of 8.91‰, and was 0.25‰ (n = 3) for the current experiment, which was comparable to the longer-term precision of 0.28‰ (n = 55) for samples analysed between October 2019 and October 2020.

For the determination of carbon-bound δ<sup>2</sup>H, samples were prepared as pairs and each individual equilibrated with one of two waters of known δ<sup>2</sup>H value, as per the method of Schuler et al. (2021). Precision of cellulose δ<sup>2</sup>H measurements was on average 2‰ (average of standard deviations for cellulose measurements in table 1 of Schuler et al., 2021). The carbon-bound δ<sup>2</sup>H of cellulose was then calculated by mass balance. Cellulose δ<sup>2</sup>H measurements were performed at the Swiss Federal Institute for Forest, Snow and Landscape Research (WSL) and all other analyses were performed at the Stable Isotope Ecology Lab, at the University of Basel.

## 2.5 | Sugar $\delta^2\text{H}$ analysis

Carbon-bound hydrogen  $\delta^2\text{H}$  of sucrose was analysed by gas chromatography-isotope ratio mass spectrometry (GC-IRMS). This required that the sucrose be derived, both to make the compound amenable to analysis by gas chromatography, and to replace hydroxyl hydrogen with hydrogen of known  $\delta^2\text{H}$  to then calculate the carbon-bound hydrogen  $\delta^2\text{H}$  from the measured whole molecule value. The procedures are described below in detail and the calculations are shown in Supporting Information 1, but in overview, a small quantity of acetic anhydride was purchased from Arndt Schimmelmann (Indiana University) with a known  $\delta^2\text{H}$  value ( $\text{AA}_{\text{Schim}}$ ;  $-133.2 \pm 2.1\text{‰}$ ) and used to acetylate pure sucrose (SIGMA Life Science, prod. No. S1888,  $\geq 99.5\%$ ) and glucose (SIGMA Life Science, prod. No. G8270, D-(+)-glucose,  $\geq 99.5\%$ ). This allowed the carbon-bound hydrogen  $\delta^2\text{H}$  of the pure sugars to be determined by mass balance. Next, aliquots of the same sugars were acetylated with acetic anhydride from the working lab stock ( $\text{AA}_{\text{lab}}$ ; SIGMA Life Science, prod. No. 320102, Lot No. STBJ5344), and the  $\delta^2\text{H}$  of these were measured. This allowed the  $\delta^2\text{H}$  of the stock acetic anhydride to be determined, which was then used to acetylate sugars in plant extracts, and for the carbon-bound hydrogen  $\delta^2\text{H}$  of the sucrose in these extracts to be calculated from the measured  $\delta^2\text{H}$  of the whole molecule.

To measure the  $\delta^2\text{H}$  of the working lab acetic anhydride, a solution ( $2 \mu\text{g} \mu\text{l}^{-1}$  concentration) of each pure sugar was made with heptane-cleaned Milli-Q water and  $50 \mu\text{l}$  was transferred to  $200 \mu\text{l}$  glass microvolume vial inserts. Three replicates were used for each sugar (glucose and sucrose) and acetic anhydride ( $\text{AA}_{\text{Schim}}$  and  $\text{AA}_{\text{lab}}$ ) combination. The sugar solution was evaporated to dryness at  $55^\circ\text{C}$  in an oven, then the samples were acetylated with  $50 \mu\text{l}$  of acetic anhydride and pyridine at  $50^\circ\text{C}$  for 2 h. The solvent was evaporated under  $\text{N}_2$ , then the samples were dissolved in acetone for quantification and  $\delta^2\text{H}$  determination.

To acetylate the extracted plant sugar, 15–30 mg of ground leaf material (that had been microwaved at harvest), was weighed into 2 ml tubes and the water-soluble compounds extracted in 1.5 ml Milli-Q water in a water bath set to  $85^\circ\text{C}$  (Lehmann et al., 2020). The tube was vortexed and centrifuged and the supernatant transferred to 20 ml glass vials using a syringe with a fitted polyethersulfone filter. All glassware used in handling organic solvents was thermally cleaned for four hrs at  $450^\circ\text{C}$  before use. The extraction was repeated giving  $\sim 3 \text{ ml}$  of extract in the 20 ml vial. The vials were placed in an oven at  $55^\circ\text{C}$  until all the water had evaporated. The dried sugar extract was then acetylated with 5 ml of  $\text{AA}_{\text{lab}}$  and 5 ml pyridine at  $50^\circ\text{C}$  for 2 h. Preliminary tests indicated that 5 ml of acetic anhydride was sufficient to ensure there was no isotope fractionation associated with incomplete sample acetylation (see Supporting Information 1). The solution was then evaporated to dryness under a gentle nitrogen gas stream, dissolved in separate aliquots of 5 ml of heptane-cleaned Milli-Q water and dichloromethane (DCM) and transferred to 15 ml glass centrifuge tubes. Acetylated sugars were recovered from the aqueous phase using three cycles of liquid-liquid extraction and centrifugation at 2000 rpm with 2:1 heptane/DCM.

The organic phase was collected in clean 20 ml glass vials, evaporated to dryness under nitrogen, transferred to 1.5 ml gas chromatography (GC) vials using DCM, then again evaporated to dryness and dissolved in acetone for GC analyses.

Concentrations of acetylated sugars were first analysed by GC-FID (flame ionization detector; Trace 1310; Thermo Fisher Scientific), and the amount of solvent adjusted to achieve around  $1.7\text{--}2 \mu\text{g}$  on column when analysed by GC-IRMS. As sucrose is the main exported sugar in all our species, we optimized the measurements for sucrose and only report on these values, despite the technique being able to resolve additional individual sugars (see Supporting Information: Figure S1.2 for examples of chromatograms). For the GC-FID and GC-IRMS analyses, samples were injected in splitless mode on a PTV (GC-FID) or split/splitless inlet on a Trace GC Ultra (GC-IRMS). Initial oven temperature was set at  $40^\circ\text{C}$  with helium carrier gas set to constant flow rate of  $1.2 \text{ ml min}^{-1}$ . After a 2 min hold at  $40^\circ\text{C}$ , the oven temperature was increased to  $140^\circ\text{C}$  at  $15^\circ\text{C min}^{-1}$ . From this point the GC-FID method was ramped to  $325^\circ\text{C}$  at  $10^\circ\text{C min}^{-1}$  and held at maximum temperature for 10 min. The GC-IRMS method increased to  $320^\circ\text{C}$  at  $8^\circ\text{C min}^{-1}$  and was held for 5 min. The GC-FID column was a GL Sciences InertCap 5 ( $30 \text{ m} \times 0.25 \text{ mm ID}$ ,  $0.25 \mu\text{m}$  column), while the GC-IRMS used a very similar Restek Rtx-5MS ( $30 \text{ m} \times 0.25 \text{ mm ID}$ ,  $0.25 \mu\text{m}$  column). For  $\delta^2\text{H}$  analyses, column effluent was converted to  $\text{H}_2$  in a pyrolysis reactor at  $1420^\circ\text{C}$  in a GC-IsoLink, and the measurement gas was introduced to a Thermo Delta V Plus IRMS for determination of the  $\delta^2\text{H}$  values. The  $\text{H}_3^+$  factor was determined at the beginning of each measurement sequence and was stable and below the manufacturer-defined threshold value over the course of all analyses.  $\delta^2\text{H}$  values were normalized to the VSMOW-SLAP scale using *n*-alkanes with known hydrogen isotopic compositions (Mix A7, purchased from Arndt Schimmelmann, Indiana University). Analytical precision for this measurement was assessed by repeated analyses of a sucrose octaacetate quality control sample, and is  $3.8\text{‰}$  ( $n = 141$ ).

The average  $\delta^2\text{H}$  of  $\text{AA}_{\text{lab}}$  determined across the three replicates of each of the two sugars was  $-194.4\text{‰}$ , with good agreement between estimates when either pure sucrose ( $-193.8 \pm 1.8\text{‰}$ ) or glucose ( $-195.1 \pm 1.2\text{‰}$ ) was used. Gaussian error propagation assuming uncorrelated errors to account for uncertainties in the two hydrogen pools indicated a combined error of  $8.5\text{‰}$  in the calculated  $\delta^2\text{H}$  value of  $\text{AA}_{\text{lab}}$ . In practice, the reproducibility was much better than this, with a standard deviation of  $1.5\text{‰}$  for two separate determinations using three replicates for each of the two sugars (i.e.,  $n = 6$ ). Thus, in this study, we use the mean  $\delta^2\text{H}$  value determined for the acetic anhydride, and report measurement uncertainty on each plant sugar as the standard deviation of the values determined for the three biological replicates.

## 2.6 | Isotope calculations

For a full summary of the isotope theory and equation derivations, please see Supporting Information 2.

Isotopic information is presented either as delta ( $\delta$ ) values and calculated as

$$\frac{R_{\text{sample}}}{R_{\text{std}}} - 1 = \delta_{\text{sample}}, \quad (1)$$

where  $R_{\text{std}}$  is the isotope ratio of VSMOW, or as enrichment above source (xylem water) water ( $\Delta$ ), which is calculated as

$$\Delta_{\text{sample}} = \frac{\delta_{\text{sample}} - \delta_{\text{XW}}}{1 + \delta_{\text{XW}}}, \quad (2)$$

where  $\delta_{\text{XW}}$  is the isotopic composition of xylem water and the subscript 'sample' refers to the measured compound.

Biosynthetic isotope fractionation ( $\epsilon_{\text{bio}}$ , including  $\epsilon_{\text{sucrose}}$ ,  $\epsilon_{\text{H}}$ , and  $\epsilon_{\text{A}}$ ), is generically defined as

$$\epsilon_{\text{compound/PW}} = \frac{R_{\text{compound}}}{R_{\text{PW}}} - 1, \quad (3)$$

where, subscript PW refers to the isotope ratio of the relevant plant water pool. All isotope parameters are scaled to ‰.

$\epsilon_{\text{A}}$  is defined as the isotopic offset between leaf extracted sugars and the relevant leaf water pool, in photosynthetically competent (sugar-exporting) cells. In the Yakir and DeNiro (1990) definition of  $\epsilon_{\text{A}}$ , the relevant sugar is triosephosphate within the chloroplast and thus reflects isotope fractionation during photosynthesis and chloroplast metabolism. The isotopic composition of the chloroplastic water is assumed to be that of leaf evaporative sites (i.e., the Craig-Gordon value; Cernusak et al., 2004). In this study, we define  $\epsilon_{\text{A}}$  further downstream from triose phosphates, to the synthesis of sucrose and distinguish  $\epsilon_{\text{A}}$  from the Yakir & DeNiro definition by  $\epsilon_{\text{sucrose}}$ . For  $\epsilon_{\text{sucrose}}$  the relevant water pool is a mixture of chloroplastic and cytosolic water (considered to be equivalent to the measurement of 'bulk' leaf water;  $\delta_{\text{LW}}$ ) depending on the extent of isotopic exchange in the cytosol. Here, we assume complete isotopic exchange with cytosolic water but we realize this is overly simplistic (see Supporting Information 4 for further details on more complex models).  $\epsilon_{\text{sucrose}}$  is then estimated as:

$$\epsilon_{\text{sucrose}} = \frac{\delta_{\text{sucrose}} - \delta_{\text{LW}}}{1 + \delta_{\text{LW}}}. \quad (4)$$

$\epsilon_{\text{H}}$  refers to the isotopic offset between the fraction of sugars that undergo isotopic exchange in sink cells and sink cell water. We take sink cell water to be the isotope composition of source (xylem) water ( $\delta_{\text{XW}}$ ), that is, we assume  $p_{\text{x}}$ , the proportion of xylem-like water in sink cells (Barbour & Farquhar, 2000), to be equal to 1 so that  $\delta_{\text{XW}} = \delta_{\text{sink cell water}}$ . For oxygen,  $\epsilon_{\text{A}}$  and  $\epsilon_{\text{H}}$  are assumed equal to the isotopic offset between carbonyl-oxygen and water,  $\epsilon_{\text{wc}}$ , of  $\approx 27\text{‰}$  (Sternberg & DeNiro, 1983; with temperature correction; Sternberg & Ellsworth, 2011). For hydrogen, the currently accepted values are those of Yakir and DeNiro (1990):  $\epsilon_{\text{A}} = -171\text{‰}$  and  $\epsilon_{\text{H}} = 158\text{‰}$ .

The cellulose isotope model is then described by a generalized two-component model:

$$\delta_{\text{cellulose}} = (1 - f)[\delta_{\text{LW}}(1 + \epsilon_{\text{A}}) + \epsilon_{\text{A}}] + f[\delta_{\text{XW}}(1 + \epsilon_{\text{H}}) + \epsilon_{\text{H}}], \quad (5)$$

where  $f$  is the fraction of oxygen or carbon-bound hydrogen in sugars that has undergone isotopic exchange during sink cell metabolism and before cellulose synthesis. Note that the second order terms in Equation (5),  $(1 + \epsilon_{\text{A}})$  and  $(1 + \epsilon_{\text{H}})$  have often been omitted within the published equations; however, for completeness and because the isotope fractionation factors tend to be large for hydrogen, we have included them.

Estimates of  $f$  can be determined from a rearrangement of Equation (5) using isotopic measurements of either oxygen or hydrogen. Subscripts, O and H are used to distinguish estimates of  $f$  for each element (i.e.,  $f_{\text{O}}$ ,  $f_{\text{H}}$ ). We used the measured values of xylem and leaf water, and leaf cellulose delta values for  $f$  calculations. For hydrogen, where  $\epsilon_{\text{A}}$  from the literature was used in the calculation (i.e.,  $-171\text{‰}$ ), we refer to the estimated  $f_{\text{H}}$  as  $f_{\text{H\_fixed}}$ , and when  $\delta^2\text{H}$  measurements of leaf sucrose are used from the studied species in place of  $\delta_{\text{LW}}(1 + \epsilon_{\text{A}}) + \epsilon_{\text{A}}$ , we refer to  $f_{\text{H}}$  as  $f_{\text{H\_variable}}$ . In both cases, for hydrogen the literature accepted value of  $\epsilon_{\text{H}}$  of  $+158\text{‰}$  was used:

$$f_{\text{H\_fixed}} = \frac{\delta_{\text{cellulose}} - \delta_{\text{LW}}(1 + \epsilon_{\text{A}}) - \epsilon_{\text{A}}}{\delta_{\text{XW}}(1 + \epsilon_{\text{H}}) - \delta_{\text{LW}}(1 + \epsilon_{\text{A}}) + \epsilon_{\text{H}} - \epsilon_{\text{A}}}, \quad (6)$$

$$f_{\text{H\_variable}} = \frac{\delta_{\text{cellulose}} - \delta_{\text{sucrose}}}{\delta_{\text{XW}}(1 + \epsilon_{\text{H}}) - \delta_{\text{sucrose}} + \epsilon_{\text{H}}}. \quad (7)$$

Refer to S2-Equation (15) (Supporting Information 2) for the derivation of Equation 7. A constant value for biosynthetic isotope fractionation implies that metabolism does not variably influence sugar  $\delta^2\text{H}$ , which is likely an over-simplification. Therefore, estimates of  $f_{\text{H}}$  should be interpreted with this limitation in mind. For oxygen, the assumption that  $\epsilon_{\text{A}} = \epsilon_{\text{H}} = \epsilon_{\text{wc}} = 27\text{‰}$ , is generally more robust, especially when considered at the level of the whole molecule (Waterhouse et al., 2002):

$$f_{\text{O}} = \frac{\delta_{\text{cellulose}} - \delta_{\text{LW}}(1 + \epsilon_{\text{wc}}) - \epsilon_{\text{wc}}}{(\delta_{\text{XW}} - \delta_{\text{LW}})(1 + \epsilon_{\text{wc}})}. \quad (8)$$

## 2.7 | Statistics

All statistical analyses were conducted in R (v4.0.3, R Core Team, 2019) with Rstudio (v1.2.1335, [www.rstudio.com](http://www.rstudio.com)). Co-variation between oxygen and hydrogen stable isotopes in xylem water, leaf water and cellulose, was investigated using standardized major axis regression with the 'sma' function in the package 'smatr' (Warton et al., 2012) (Figure 1), whereas correlations between dependent and independent variables were explored using ordinary least squares regression with the 'lm' function in the base R package 'stats' (Figures 2, 4–6). Least squares means for species trait values were estimated using 'aov' function, with significant differences determined using 'TukeyHSD'; both from the base R package 'stats' (Figure 3).

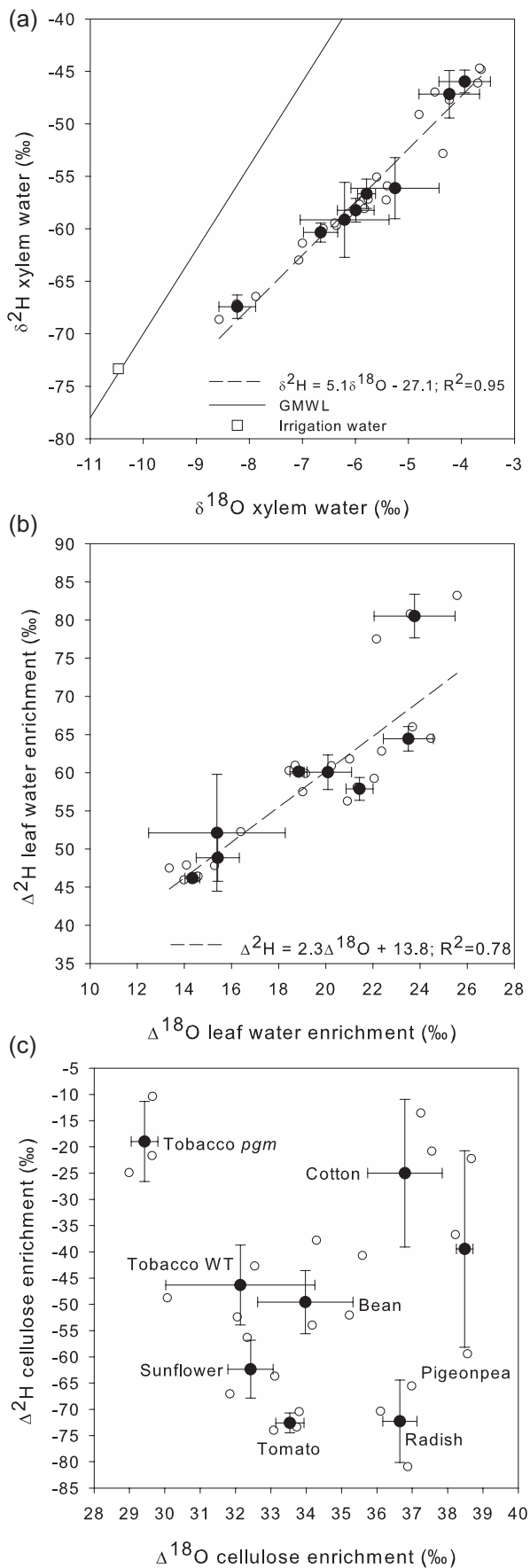


FIGURE 1 (See caption on next page)

### 3 | RESULTS

#### 3.1 | Coordination between oxygen and hydrogen isotope composition is lost in cellulose

Despite the eight species and mutant having been grown under the same controlled environment conditions, there was substantial isotopic variation in xylem water (species average range:  $-67.4\%$  to  $-46.0\%$  for H;  $-8.2\%$  to  $-3.9\%$  for O), leaf water enrichment above xylem water ( $46.2\%$  to  $80.5\%$  for H;  $14.3\%$  to  $23.8\%$  for O) and cellulose enrichment above xylem water ( $-72.6\%$  to  $-19.0\%$  for H;  $29.4\%$  to  $38.5\%$  for O) (Figure 1; see also Supporting Information: Table S5.4 for all isotopic data from individuals). Moreover, significant differences between species were found for each of these variables (see Supporting Information: Table S5.5). We used this variation to assess the extent of coordination between the two elements.

Compared to irrigation water ( $\delta^2\text{H} = -73.3\%$ ,  $\delta^{18}\text{O} = -10.5\%$ ), water extracted from root crowns was both  $^2\text{H}$  and  $^{18}\text{O}$  enriched with deviation from the meteoric water line in a bi-plot of  $\delta^2\text{H}$  versus  $\delta^{18}\text{O}$  (Figure 1a). Removing isotopic variation in xylem water, leaf water was evaporatively  $^2\text{H}$  and  $^{18}\text{O}$  enriched, as expected, with species variation observed (Supporting Information: Table S5.5); however, the  $R^2$  was 0.78 for the bi-plot of  $\Delta^2\text{H}$  versus  $\Delta^{18}\text{O}$  of leaf water (Figure 1b;  $p < 0.001$ ) compared with 0.95 for the biplot of  $\delta^2\text{H}$  versus  $\delta^{18}\text{O}$  of xylem water (Figure 1a;  $p < 0.001$ ). Assuming constant biosynthetic isotope fractionation factors for oxygen and carbon-bound hydrogen, the correlation between isotope compositions of the two elements in cellulose should have been comparable to plant water. However, as shown in Figure 1c, there was no correlation.

#### 3.2 | Source leaf isotope effects explain the majority of $\delta^2\text{H}$ cellulose variation

Measuring leaf sugar  $\delta^2\text{H}$  allowed us to separate the influence of source (pre-sucrose export from photosynthesizing mature leaves) and sink (post-sucrose import into developing leaf tissue) isotope effects on the  $\delta^2\text{H}$  of cellulose using Equation 5. Overall, 66% of the variation in cellulose carbon-bound hydrogen  $\delta^2\text{H}$  was explained by source sucrose  $\delta^2\text{H}$  values ( $R^2 = 0.66$ ; Figure 2a;  $p < 0.001$ ). There was no correlation between sucrose  $\delta^2\text{H}$  and leaf water  $\delta^2\text{H}$  (inset Figure 2b;  $p > 0.05$ ); meaning, sucrose  $\delta^2\text{H}$  variation was driven by species differences in the isotopic offset between sucrose and leaf water ( $\epsilon_{\text{sucrose}}$ ) (Figures 2b and 3a).  $\epsilon_{\text{sucrose}}$  was less negative than the assumed value of  $-171\%$  in all species except radish, which had a least squares mean value of  $-192\%$  (s.e.  $5.7\%$ ).

Sink cell isotope effects include both the fraction of carbon-bound H that exchanges with local water ( $f_{\text{H}}$ ) and biosynthetic isotope fractionation ( $\epsilon_{\text{H}}$ ). In this study, we were unable to quantify  $\epsilon_{\text{H}}$  and used the assumed constant value of  $+158\%$ . Therefore, the remaining 34% of the variation associated with sink cell processes (and unexplained variation) in Figure 2, was attributed to variation

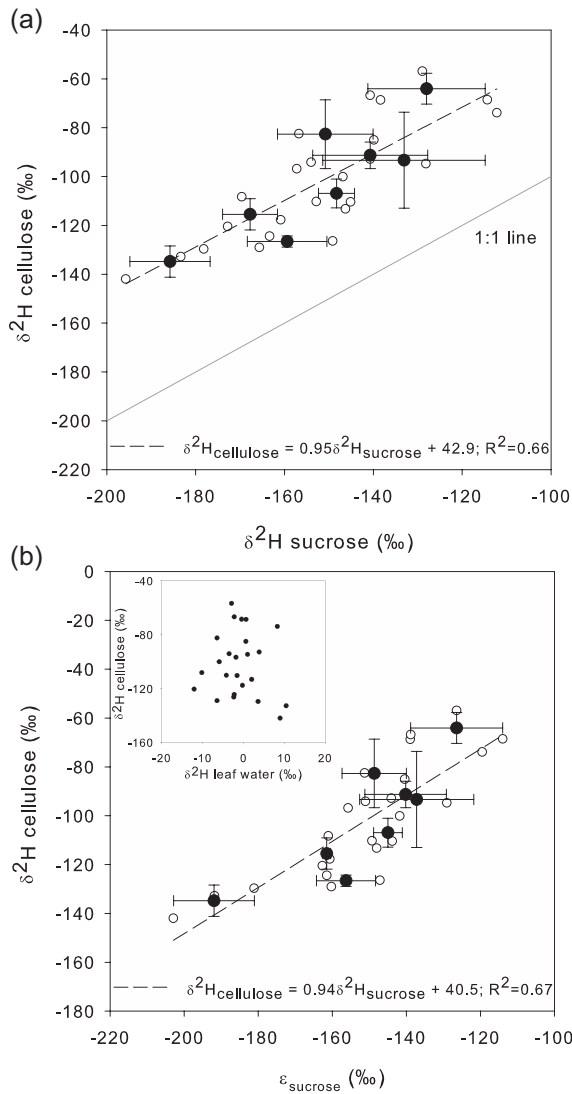


**FIGURE 2** Isotopic predictors of leaf cellulose  $\delta^2\text{H}$ : (a) sucrose  $\delta^2\text{H}$ , and (b)  $\epsilon_{\text{sucrose}}$ . Inset in (b) shows there is no relationship between  $\delta^2\text{H}$  leaf water and  $\delta^2\text{H}$  cellulose in this study. As such, sucrose  $\delta^2\text{H}$  variation is driven by species differences in  $\epsilon_{\text{sucrose}}$ . Individual plant values are shown by the white circles; means are shown by the black circles with standard deviation used for the error bars ( $n = 3$  per species). Dashed regression lines are significant ( $p < 0.05$ ) and fitted by ordinary least squares regression. Slopes are non-significantly different from 1, and intercepts, not significantly different from zero.

in  $f_{\text{H}}$  (Figure 3b) and xylem water  $\delta^2\text{H}$  differences. Because  $\epsilon_{\text{H}}$  is large and positive, even though xylem water is  $^2\text{H}$ -depleted compared to leaf water, isotopic exchange results in cellulose being enriched in  $^2\text{H}$  above source sucrose; as confirmed by the

**FIGURE 1** Coordination between oxygen and hydrogen stable isotopes in (a) xylem water, (b) leaf water enrichment and (c) cellulose enrichment. Individual plant values are shown by the white circles; means are shown by the black circles with standard deviation used for the error bars ( $n = 3$  per species). Dashed regression lines are significant ( $p < 0.05$ ) and fitted by standardized major axis regression. For reference, the global meteoric water line (GMWL) is given in (a).

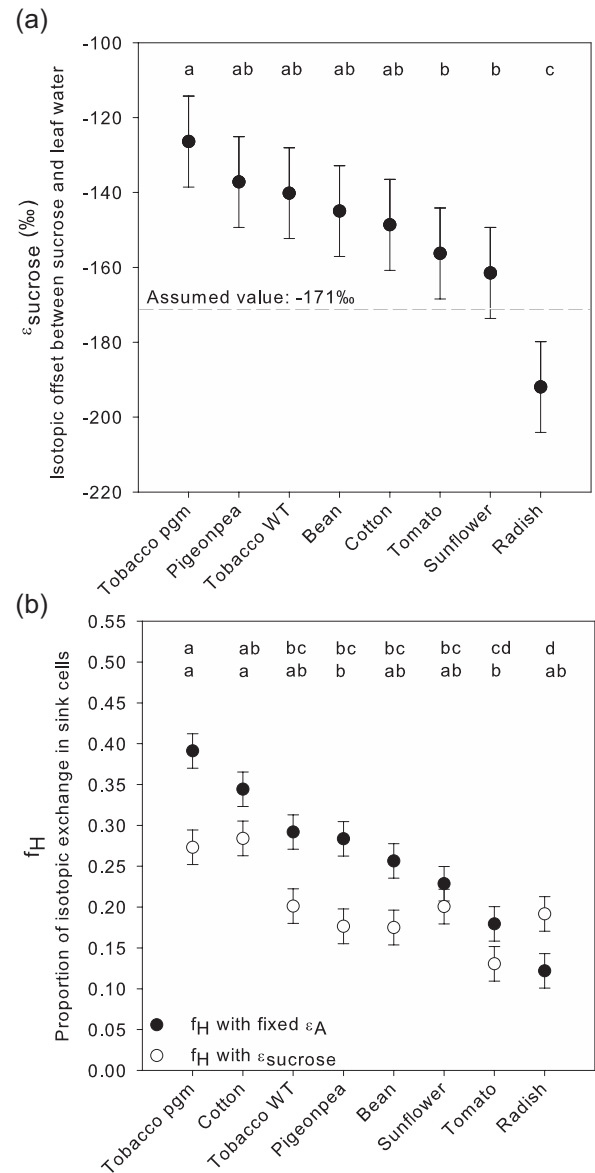


**FIGURE 3** Species variation in source leaf and sink cell isotope effects: (a)  $\epsilon_{\text{sucrose}}$  calculated according to Equation (4) utilizing sucrose and leaf water  $\delta^2\text{H}$  information, with the assumed value of  $-171\text{‰}$  provided for reference and, (b)  $f_{\text{H}}$  estimated assuming fixed  $\epsilon_{\text{A}}$  of  $-171\text{‰}$  (Equation 6) or variable  $\epsilon_{\text{sucrose}}$  estimated from sucrose  $\delta^2\text{H}$  (Equation 7). Significant differences are given by the letters. In (b) the top line of letters is associated with the black circles and the bottom line, the white circles. 95% confidence limits are given as the error around the least squares means ( $n = 3$  per species).

positive intercept in Figure 2a.  $f_{\text{H}}$  was estimated assuming either a fixed  $\epsilon_{\text{A}}$  of  $-171\text{‰}$  (Equation 6;  $f_{\text{H\_fixed}}$ ) or variable  $\epsilon_{\text{sucrose}}$  calculated from sucrose  $\delta^2\text{H}$  measurements (Equation 7;  $f_{\text{H\_variable}}$ ). Given that species variation in  $\epsilon_{\text{sucrose}}$  was observed (Figure 3a), differences among species were smaller for  $f_{\text{H\_variable}}$  compared with  $f_{\text{H\_fixed}}$  (Figure 3b). Furthermore, because species values of  $\epsilon_{\text{sucrose}}$  were generally higher than  $-171\text{‰}$ , estimates of  $f_{\text{H\_variable}}$  were lower than those of  $f_{\text{H\_fixed}}$ . Assuming a  $\epsilon_{\text{A}}$  and  $\epsilon_{\text{H}}$  of  $27\text{‰}$  for

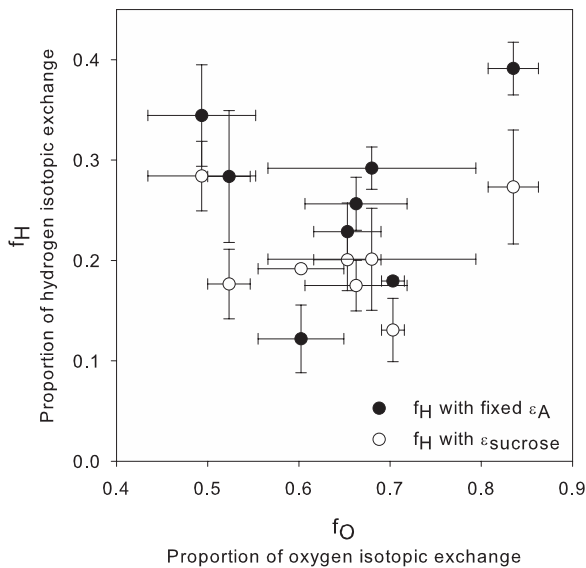


**FIGURE 4** Relations between the proportion of carbon-bound hydrogen that undergoes isotopic exchange in sink cells ( $f_H$ ) estimated assuming fixed  $\epsilon_A$  of  $-171\text{‰}$  (Equation 6) or variable  $\epsilon_{\text{sucrose}}$  estimated from sucrose  $\delta^2\text{H}$  (Equation 7), and the proportion of oxygen that undergoes isotopic exchange in sink cells ( $f_O$ ). Standard deviation used for the error bars ( $n = 3$  per species).

oxygen,  $f_O$  estimates were also calculated and species-specific differences also observed (species mean range of 0.49–0.84; Supporting Information: Figure S5.1). However, there was no correlation between  $f_H$  and  $f_O$  estimates ( $p > 0.05$ ; Figure 4).

### 3.3 | Relationships between model parameters and metabolic proxies

Metabolic effects on isotope fractionation include variation in the partitioning of carbon between branch points and the absolute flux through the pathway. Assimilation rate was taken as a proxy measure of the overall flux through triose-phosphates; dark respiration rate as a proxy measure of glycolytic activity; the turnover time of sugars ( $\tau$ ) as a proxy for the length of time available for metabolites to cycle via triose–hexose phosphates and undergo isotopic exchange with local water; and, the proportion of sugars [sugars/(sugars+starch)] taken as a proxy for the partitioning between sucrose and starch. Of these measures,  $\epsilon_{\text{sucrose}}$  was positively related to dark respiration ( $R^2 = 0.27$ ;  $p < .01$ ; Figure 5),  $\tau$  ( $R^2 = 0.35$ ;  $p < 0.01$ ; Figure 6a) and the proportion of sugars ( $R^2 = 0.27$ ;  $p < 0.05$ ; Figure 6b), but only weakly negatively related to assimilation rate ( $R^2 = 0.19$ ;  $p < 0.05$ ; Supporting Information: Figure S5.2).

The strength of the relationships between  $f_H$  and the relevant metabolic proxies were weakened, but remained significant when  $f_H$  was estimated using  $\epsilon_{\text{sucrose}}$  compared with when  $f_H$  was estimated with fixed  $\epsilon_A$  of  $-171\text{‰}$  (Figure 6c,d).  $f_{H\_variable}$  was positively related to  $\tau$  ( $R^2 = 0.17$ ;  $p < 0.01$ ; Figure 6c) and sugar

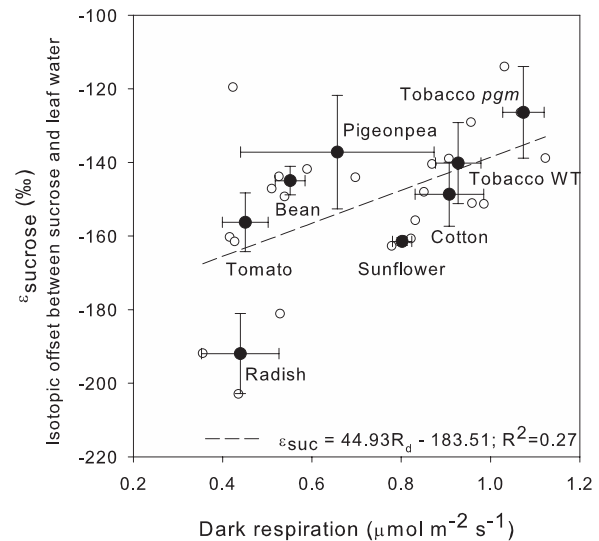


**FIGURE 5**  $\epsilon_{\text{sucrose}}$  in relation to dark respiration.  $\epsilon_{\text{sucrose}}$  estimated according to Equation (4). Individual plant values are shown by the white circles; means are shown by the black circles with standard deviation used for the error bars ( $n = 3$  per species). Regression line is significant ( $p < 0.05$ ) and fitted by ordinary least squares regression.

partitioning ( $R^2 = 0.28$ ;  $p < 0.001$ ; Figure 6d); however, in the latter case, the strength of the relationship was dependent on the tobacco *pgm* mutant (without, the  $R^2 = 0.10$ ;  $p > 0.05$ ), as was similarly the case for  $\epsilon_{\text{sucrose}}$  (without tobacco *pgm*, the  $R^2 = 0.02$ ;  $p > 0.05$ ). There was also, no relation between  $f_O$  and  $\tau$  ( $R^2 = 0.08$ ;  $p > 0.05$ ; data not shown).

## 4 | DISCUSSION

One of the main purposes of developing semi-mechanistic models of cellulose isotopic variation, is to be able to invert the model to estimate parameters of interest, which are retrospectively difficult to assess. For example, the cellulose isotope models have been used to infer leaf temperature (Helliker & Richter, 2008); deuterium deviations (as a proxy for relative humidity) (Voelker et al., 2014); stomatal conductance induced changes in water-use efficiency (Guerrieri et al., 2019); origin of plant material (Cueni et al., 2021); and, source of water for trees (Sargeant et al., 2019); as well as estimate the fraction of isotopic exchange in sink cell water (e.g., Cheesman & Cernusak, 2016; Song et al., 2014). However, to perform these calculations, the values of isotopic exchange and/or biosynthetic isotope fractionation are generally assumed constant across species and environmental conditions. In this study, we directly measured carbon-bound hydrogen  $\delta^2\text{H}$  of plant extracted sucrose and found species variation in biosynthetic isotope fractionation during sucrose synthesized in mature photosynthesizing leaves;  $\epsilon_{\text{sucrose}}$  (Figure 3a). We discuss the implications of these results in terms of metabolic drivers and subsequent

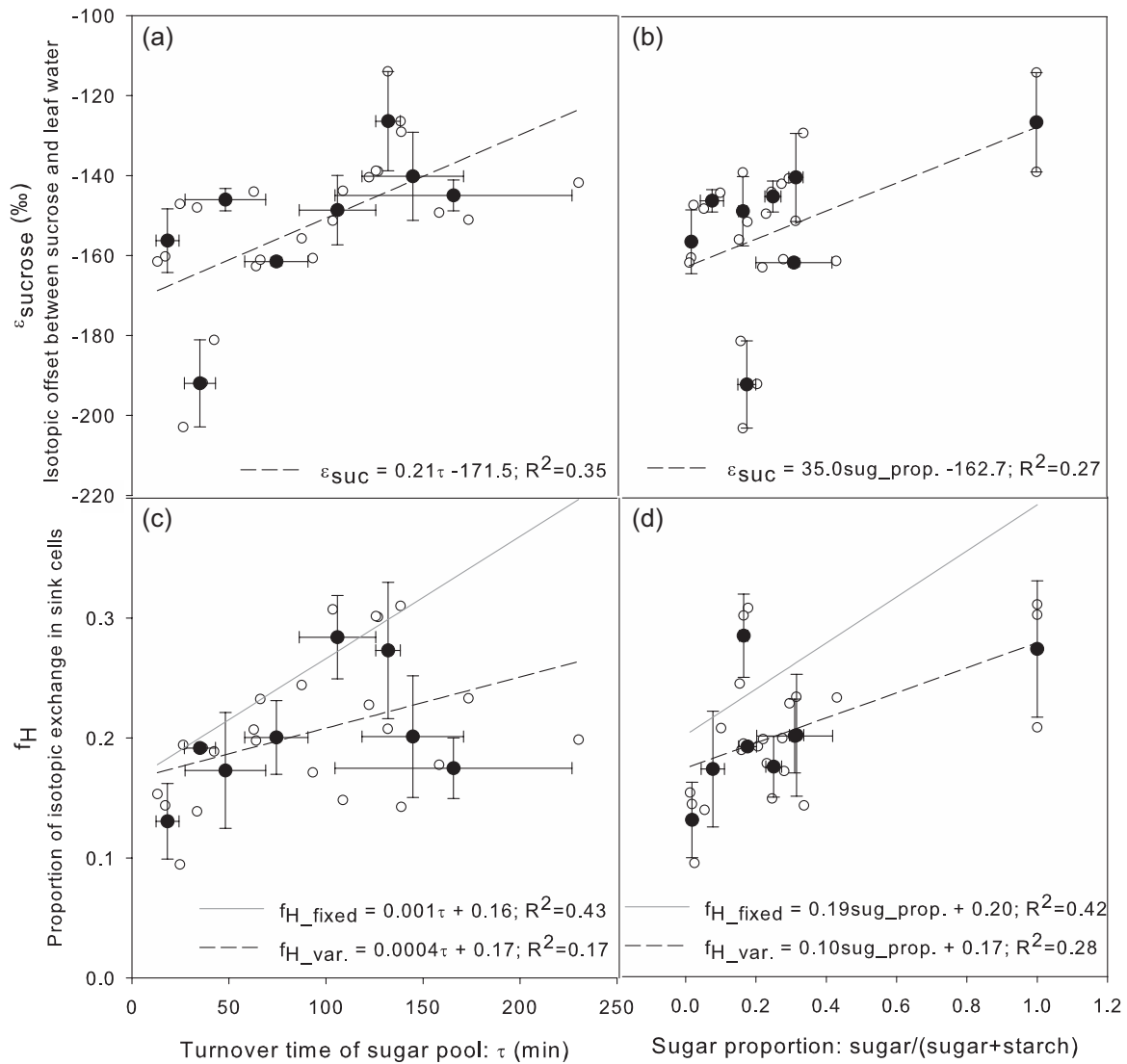


**FIGURE 6** Sources of isotopic variation and their relation to metabolic proxies including sugar turnover time (a and c) and the proportion of sugar in source leaves (b and d) for  $\epsilon_{\text{sucrose}}$  estimated according to Equation (4); and,  $f_H$  estimated assuming either fixed  $\epsilon_A$  of  $-171\text{‰}$  ( $f_{H\_fixed}$ ; grey, solid regression lines; individual values not shown) or using  $\epsilon_{\text{sucrose}}$  ( $f_{H\_var.}$ ; dashed, black regression lines). Individual plant values, for  $\epsilon_{\text{sucrose}}$  and  $f_{H\_var.}$ , are shown by the white circles; means are shown by the black circles with standard deviation used for the error bars ( $n = 3$  per species). Regression lines are significant ( $p < 0.05$ ) and fitted by ordinary least squares regression.

estimation and interpretation of isotopic exchange ( $f_H$ ). In conclusion we highlight the need to consider alternative source-sink scenarios of cellulose synthesis if we are to interpret cellulose isotopic variation with respect to changes in plant metabolism.

#### 4.1 | A loss of coordination between $\Delta^{18}\text{O}$ and $\Delta^2\text{H}$ in cellulose suggests one or more of the model parameters varies across species

To test whether parameter values in the cellulose isotope models are constant, we assessed coordination between cellulose oxygen and hydrogen isotopes. This is on the basis that cellulose derives oxygen and hydrogen from plant water, for which a linear relationship between the

two elements is expected (Craig & Gordon, 1965; Farquhar & Lloyd, 1993). Indeed, the isotopic composition of oxygen and hydrogen were strongly related in xylem water (Figure 1a). For the isotopic composition of leaf water, we assessed coordination on an enrichment basis, which removes the influence of variation in the isotopic composition of xylem water and therefore captures the expected relationship between elements based on isotope fractionation during transpiration (Cernusak et al., 2016). Taking the average daytime temperature of  $26.2^\circ\text{C}$  as representative of leaf temperature, the theoretical slope of  $\Delta^2\text{H}$  versus  $\Delta^{18}\text{O}$  in leaf water should have been  $\approx 3.03$ , assuming the vapour was in equilibrium with source water. Deviation from the theoretical slope (ratio of kinetic and equilibrium fractionation factors) and variation around the line in Figure 1b, suggests that (i) leaf temperature varied across species influencing the ratio of atmospheric to internal vapour pressure

( $e_a/e_s$ ); (ii) that the water vapour was not in equilibrium with soil water; and/or, (iii) the pathlength that influences the extent to which bulk leaf water is  $^2\text{H}$  or  $^{18}\text{O}$  depleted relative to the estimated value at evaporative sites (the Péclet effect; Farquhar & Lloyd, 1993), differed between species (e.g., Kahmen et al., 2008). However, as the coefficient of determination for leaf water enrichment was still generally high ( $R^2=0.78$ ; Figure 1b), this does not explain the complete loss of coordination between oxygen and hydrogen isotopes found for cellulose enrichment (Figure 1c). Therefore, one or more of the model parameters in either (or both) the oxygen and/or hydrogen cellulose isotope models likely varied across species.

## 4.2 | Are species-specific differences in $\epsilon_{\text{sucrose}}$ driven by metabolism or apparent due to experimental limitations?

In measuring the  $\delta^2\text{H}$  of sucrose, 66% of the cellulose isotopic variation could be explained by variation in the expression of source-leaf isotope effects ( $R^2=0.66$ ; Figure 2a). Importantly, leaf water variation explained minimal cellulose isotopic variation and was instead explained by isotope fractionation during sugar metabolism ( $\epsilon_{\text{sucrose}}$ ) (Figure 2b). Significant differences in  $\epsilon_{\text{sucrose}}$  among species were observed (Figure 3a), with all except radish having values higher than the literature assumed value of  $-171\text{‰}$ . This makes sense as, in the original conceptualization of the cellulose isotope model by Yakir and DeNiro (1990),  $\epsilon_A$  was hypothesized to reflect biosynthetic isotope fractionation only associated with the production of triose-phosphates in the chloroplast during photosynthesis and not further downstream to the production of sucrose as we do here.

Variation in the isotopic composition of the NADPH pool is often suggested to be the cause of cellulose  $\delta^2\text{H}$  variation on account of the negative relations found between cellulose  $\delta^2\text{H}$  and electron transport rate (Sanchez-Bragado et al., 2019), and growth (Lehmann et al., 2021). We too, found a similar albeit weak negative correlation between  $\epsilon_{\text{sucrose}}$  and assimilation rate (Supporting Information: Figure S5.2). However, the dramatic  $^2\text{H}$ -depletion associated with reactions in the chloroplast, is unlikely to be the source of variation in  $\epsilon_{\text{sucrose}}$  as the reduction of  $\text{NADP}^+$  by the photosynthetic machinery (ferredoxin-NADP oxidoreductase) is effectively irreversible (the free proton pool is unlikely to be limited so that the kinetic isotope effect is always 'fully' expressed). Instead, the association with assimilation rate is perhaps more representative of the overall flux through triose-phosphates, where the larger the flux, the faster the turnover of triose-phosphates in the cytosol. As such, we hypothesize that variation in  $\epsilon_{\text{sucrose}}$  may reflect isotope fractionation in the cytosol before the export of sucrose, due to  $^2\text{H}$ -enrichment in intermediates of sugar metabolism (Yakir & DeNiro, 1990). In support of this idea,  $\epsilon_{\text{sucrose}}$  was found to be  $-171.5 \pm 6.7\text{‰}$  when the turnover of sugars was zero (intercept of Figure 6a).

In addition, isotope fractionation associated with the major branch points from triose-phosphate in the chloroplast including sucrose synthesis, glycolysis and starch synthesis, has the potential

to influence the remaining triosephosphate pool (reflected in variability of  $\epsilon_A$ ) and hence the resulting sucrose  $\delta^2\text{H}$  (reflected in variability of  $\epsilon_{\text{sucrose}}$ ). In that regard, it is interesting to note the moderately strong positive relationship between  $\epsilon_{\text{sucrose}}$  and night time respiration (Figure 5a) and starch partitioning (Figure 6b). Ultimately, a detailed assessment of metabolic fluxes would be required to confirm the relative influence of each pathway (e.g., Wijker et al., 2019).

An alternative and non-mutually exclusive hypothesis is that the variation in  $\epsilon_{\text{sucrose}}$  reflects an apparent isotope effect rather than the result of metabolic differences between species. Such an apparent isotope effect may occur if (i) the bulk leaf water  $\delta^2\text{H}$  which is used to estimate  $\epsilon_{\text{sucrose}}$ , is not representative of the water pool where hydrogen isotope effects occur; and/or (ii) the turnover time of leaf water is much faster than that of leaf sugar.

With respect to point (i), de novo synthesized triose-phosphate occurs within chloroplastic water, which is assumed to have an isotope composition equal to that of evaporative sites (Craig-Gordon delta value) (Cernusak et al., 2004). In contrast, the isotope composition of cytosolic water, where subsequent carbon-bound hydrogen isotope exchange reactions occur, is assumed to be represented by bulk leaf water measurements with major veins removed (Barbour et al., 2000; Cernusak et al., 2002). Thus, depending on the extent of carbon-bound hydrogen isotope exchange in the cytosol, the reference value for the source of hydrogen associated with  $\epsilon_A$  effects in sucrose, may be somewhere between the  $\delta^2\text{H}$  values of these two water pools. A further complication is the spatial distribution of sucrose synthesis and export, which may not be even across the leaf surface. This has been proposed to be of particular importance in interpreting  $\delta^{18}\text{O}$  patterns of leaf sugar in grasses (Baca Cabrera et al., 2021; Lehmann et al., 2017 preprint). Finally, artefacts in the cryogenic extraction approach for measuring the isotopic composition of plant water have recently been described (Chen et al., 2020); although the extent of the isotopic offset associated with the proposed hydrogen isotope exchange between carbon-bound hydrogen and liquid water during distillation has not yet been tested in leaf or root material.

With respect to point (ii), we did not measure the water content of leaves to make direct estimates of leaf water turnover time. However, if we assume that the relative water content is 90%, using the measurements of specific leaf area and transpiration rate, we can make approximate estimates. When we did this, we noted that the turnover time for leaf water in half of the species is faster than the turnover time for sugars, by on average 75 min (Supporting Information: Table S5.1). This means that if the leaf water isotope composition was subject to change, deviation from  $-171\text{‰}$  could reflect a mismatch between isotopic integration times. Faster turnover times for water compared with sugar are in line with Lehmann et al. (2020) and may also partially explain the isotopic disequilibrium between the measured leaf water and sugar when grasses were grown under different relative humidity conditions (and hence transpiration rates leading to different leaf water turnover times) (Lehmann et al., 2017). All this is to say that comparing

estimates of biosynthetic fractionations may be biased depending on the reference leaf water pool used. Disequilibrium is likely to be more apparent in field investigations than in controlled environment conditions, but growing plants at high humidity and with the vapour in isotopic equilibrium with source water can help to minimize diurnal deviation in the leaf water  $\delta^2\text{H}$  and the isotope gradient between evaporative sites and xylem water. That said, estimates of  $f_{\text{H}}$  remain robust when  $\delta_{\text{sucrose}}$  is used in Equation (7) ( $\delta_{\text{sucrose}} = \delta_{\text{LW}}(1 + \epsilon_{\text{A}}) + \epsilon_{\text{A}}$ ), as this does not require an assumption of the source leaf water pool; however, it remains an issue for our estimates of  $f_{\text{O}}$  as we did not similarly measure the  $\delta^{18}\text{O}$  of leaf sucrose.

### 4.3 | Interpreting variation in $f_{\text{O}}$ and $f_{\text{H}}$ estimates

When observed values of  $\epsilon_{\text{sucrose}}$  were used, there was less variation in  $f_{\text{H}}$ , compared with  $f_{\text{H}}$  values estimated using a fixed  $\epsilon_{\text{A}}$  value of  $-171\text{‰}$  (Figure 3b). In turn, the relationship between  $f_{\text{H}}$  and sugar turnover time was weakened (Figure 6c). There was also no relation between  $f_{\text{O}}$  and turnover time, as expected (data not shown). Compared with the study of Song et al. (2014) where variation in  $f_{\text{O}}$  and turnover time was achieved by growing one species under different conditions, we rely here on species differences. This suggests that the interpretation of  $f_{\text{H}}$  and  $f_{\text{O}}$  variability may not be universal across species. As approximated here and in Song et al. (2014) sugar turnover time is only indirectly related to metabolite cycling on the basis that the slower the turnover of the sugar pool, the more opportunity for sugars to cycle and therefore undergo isotopic exchange. Thus, ideally, more direct measures of triose-hexose phosphate cycling (e.g., Hill et al., 1995) are required to confirm the metabolic link to estimates of isotopic exchange.

Whilst there is empirical support for proportionality between  $f_{\text{O}}$  and  $f_{\text{H}}$  (Luo & Sternberg, 1992), and metabolite cycling through triose-hexose conversion reactions underpins both parameters, the lack of correlation found in this study (Figure 4) could be explained due differences in the mechanisms of isotopic exchange between elements and complexities such as disequilibrium (Barbour, 1999; Farquhar et al., 1998) or intramolecular hydrogen transfer (without exchange with water) (e.g., PGI: Rose & O'Connell, 1961; TPI: O'Donoghue et al., 2005a, 2005b). These effects are not captured within the simplified expression of the isotopic composition of sugar, that is, oxygen and carbon-bound hydrogen originating from one of two water pools with assumptions on the kinetic and equilibrium isotope effects during sugar metabolism. Another nonexclusive possibility is disequilibrium between *de novo* sucrose and sucrose derived from transitory stores of starch, which may be exacerbated by differences in diel growth patterns between species. When triose-phosphate is directed to starch synthesis, a large  $^2\text{H}$ -depletion in starch relative to sucrose has been observed in  $\text{C}_3$  plants (Schuler et al., 2021), owing to disequilibrium of chloroplastic PGI, which  $^2\text{H}$ -depletes glucose-6-phosphate relative to fructose-6-phosphate (Schleucher et al., 1999). Our point-in-time measurements of the

isotopic composition of leaf water and sucrose assume sugars that supply cellulose synthesis carry the isotopic composition of daytime conditions, despite sucrose export and cellulose deposition not being limited to the day. Furthermore, fluxes through cytosolic metabolic pathways are altered between day and night on account of sugar export from the chloroplast being in the form of triose-phosphate during the day, but at night, degraded starch products include glucose and maltose (Weise et al., 2004). Thus, a variable contribution of night-time sucrose from starch could impact downstream estimates of  $f_{\text{H}}$ , if diurnal variation in  $\epsilon_{\text{sucrose}}$  is not considered. It is unknown if similar isotope effects between starch and sucrose can be considered for  $\delta^{18}\text{O}$ ; however, as  $^{18}\text{O}$  isotope fractionation is generally smaller than for hydrogen, any effect on  $f_{\text{O}}$  estimates will likely be smaller. We consider the isotope effects of diurnal sucrose and nocturnal growth in Supporting Information 3.

### 4.4 | Consequence of sucrose-starch partitioning on isotopic exchange in sink cells

Besides the impact of sucrose-starch partitioning on the diurnal isotopic composition of sucrose in source leaves, there may also be effects on isotopic exchange in sink cells, linked to futile cycling of sugars. Considering starch partitioning as an important integrator of carbon metabolism and growth (Stitt & Zeeman, 2012; Sulpice et al., 2009), we hypothesized, all else being equal, that for a given sink strength (relative growth rate of sink organs), if the flux towards sucrose synthesis is small relative to that of starch, the sucrose pool may be small and thus the residence time of sucrose in sink cells would be too short to allow for substantial metabolite cycling and hence isotopic exchange. Conversely, if growth is slow relative to exported sucrose, then there may be greater opportunity for triose-hexose futile cycling in sink tissue. In fact, we did find a positive relationship of  $f_{\text{H}}$  with the proportion of sugars in source leaves (Figure 6d). However, the strength of the relation was highly influenced by tobacco *pgm*. This mutant, which is almost unable to synthesize starch (sucrose partitioning of one), had higher  $f_{\text{H}}$  and  $f_{\text{O}}$  values compared with the WT (however, not significantly different:  $f_{\text{H}}$ ; Figure 3b;  $f_{\text{O}}$ : Supporting Information: Figure S5.1). Still, the comparison between WT and mutant serves as a useful model to look at the influence of altered sucrose-starch partitioning on isotope fractionation (Lehmann et al., 2019).

Based on the work in *Arabidopsis thaliana*, reduced carbon flow into starch results in more carbon channelled into sugars and exported to sink regions (Kölling et al., 2015). Specifically, in tobacco *pgm*, the amount of carbon stored as sugars in the vacuole may be equivalent to that of starch stored in WT chloroplasts, explaining why growth is not severely impacted in tobacco *pgm* compared with other species of the same mutation such as *A. thaliana pgm* (Hanson & McHale, 1988). As hexoses tend not to accumulate, 'sucrose-cycling' between sucrose and hexoses has been suggested (Huber, 1989). Importantly, this cycle may

interact with the substrate cycle between triose-hexose phosphates (Dancer et al., 1990; Hatzfeld & Stitt, 1990) thus facilitating isotopic exchange. Functionally, the interaction between these two futile cycles may be required to adapt the flux through the sucrose pool to changes in source-sink activity (e.g., Amthor et al., 2019). Incidentally, sucrose-cycling is also observed in leaves (e.g. Huber, 1989). Since futile cycles consume ATP (Alonso et al., 2005), this may explain the link between  $\epsilon_{\text{sucrose}}$  and respiration rate (Figure 5a). In future studies, estimates of the flux of exported sugar (e.g., Kölling et al., 2015) relative to cellulose deposition (e.g., Ivakov et al., 2017) may help to validate the ideas presented here and guide the metabolic interpretation of variation in isotopic exchange.

#### 4.5 | Perspectives to understand cellulose isotope variation

Taken as a whole, our results suggest that  $\epsilon_{\text{sucrose}}$  may not be constant, which will impact on the use of the cellulose isotope model to solve for parameters of interest, including  $\delta_{\text{LW}}$ ,  $\delta_{\text{XW}}$ , and  $f_{\text{H}}$ . Moreover, we have highlighted a number of conceptual and experimental shortcomings that currently limit the interpretation of model parameters within a physiological context. For oxygen, we did not assess  $\epsilon_{\text{sucrose}}$  variability, and for hydrogen we still assumed the estimate of  $\epsilon_{\text{H}}$  to be invariant at 158‰ (if  $\epsilon_{\text{H}}$  is instead allowed to vary and  $f_{\text{H}}$  held constant, there is negative compensation between  $\epsilon_{\text{H}}$  and  $f_{\text{H}}$ ; Supporting Information: Figure S5.4). In Supporting Information 4, we progress the ideas presented here by providing an approach to estimate  $f_{\text{H}}$ ,  $\epsilon_{\text{H}}$ , and  $\epsilon_{\text{A}}$  within the one experiment, by growing plants with different isotopic waters. Of importance will be determining whether  $\epsilon_{\text{sucrose}}$  varies diurnally and whether this is an apparent effect associated with different turnover times of leaf water and sugar pools, or associated with diel metabolic changes. Assimilation-weighting  $\delta_{\text{sucrose}}$  has previously been suggested as a more accurate determination of the isotopic composition of exported sugar (Cernusak et al., 2005). However, preferably, export-weighting  $\delta_{\text{sucrose}}$  to sink cells or growth-weighting (assuming homeostatic sugar concentrations in sink cells, that is, what is going out is coming in), would help capture nocturnal effects. Ideally, time varying metabolic isotope models that capture fluxes and reservoir sizes would be helpful for exploring plausible mechanisms (e.g., Hirl et al., 2021; Wijker et al., 2019). Growing plants under different photo-periods (Sulpice et al., 2014), may help elucidate whether sucrose derived from starch and nocturnal growth is of significance to interpreting isotopic variation in cellulose (Supporting Information 3). The impact of night-time starch degradation and export on the isotopic composition of translocated photosynthate is just one example of complexity, that to date, has not been adequately considered (Gessler et al., 2007). The temporal and spatial location of biosynthetic steps and the different isotopic composition of the water pools where they occur was recently investigated utilizing banana leaves where part of the leaf is synthesized heterotrophically

(Zhu et al., 2020). In Supporting Information 4 we also consider a number of different leaf tissue growth scenarios than the one represented by the current isotope model (Model 1). For progressing the cellulose hydrogen isotope model, it is apparent that our current approach of assuming constant parameter values is insufficient, but with the additional information provided by  $\delta^2\text{H}$  of sugars, progress in our understanding of cellulose  $\delta^2\text{H}$  variation is possible, allowing for robust interpretation.

#### ACKNOWLEDGEMENTS

We thank Samuel Zeeman (ETH Zurich) for kindly providing the tobacco WT and mutant seeds, Santiago Pérez-Bernal (Uni Basel) for the pigeonpea seeds, Siro Ellenberger (Uni Basel) for the NSC analysis, and Manuela Oetli for technical support in the  $\delta^2\text{H}$  analysis of cellulose (WSL). Many thanks also to two anonymous reviewers for their keen interest and suggestions that helped improve this manuscript. The authors acknowledge the funding support from the European Research Council (ERC) under the European Union's Horizon 2020 research and innovation programme (grant agreement No. 724759). MML was funded by the SNSF Ambizione grant (No. 179978) and G. T. thanks the support of the *Région Pays de la Loire* and *Angers Loire Métropole* via the grant Connect Talent Ioseed. Open access funding provided by Universitat Basel.

#### DATA AVAILABILITY STATEMENT

The data that support the findings of this study are available from the corresponding author upon reasonable request.

#### ORCID

Meisha Holloway-Phillips  <http://orcid.org/0000-0002-8353-3536>

Jochem Baan  <https://orcid.org/0000-0003-3955-3262>

Daniel B. Nelson  <https://orcid.org/0000-0002-2716-7770>

Marco M. Lehmann  <https://orcid.org/0000-0003-2962-3351>

Guillaume Tcherkez  <http://orcid.org/0000-0002-3339-956X>

Ansgar Kahmen  <https://orcid.org/0000-0002-7823-5163>

#### REFERENCES

- Alonso, A.P., Vigeolas, H., Raymond, P., Rolin, D. & Dieuaide-Noubhani, M. (2005) A New Substrate Cycle in Plants. Evidence for a High Glucose-Phosphate-to-Glucose Turnover from in Vivo Steady-State and Pulse-Labeling Experiments with  $[13\text{C}]$ Glucose and  $[14\text{C}]$ Glucose. *Plant Physiology*, 138(4), 2220–2232. <https://doi.org/10.1104/pp.105.062083>
- Amthor, J.S., Bar-Even, A., Hanson, A.D., Millar, A.H., Stitt, M., Sweetlove, L.J. et al. (2019) Engineering strategies to boost crop productivity by cutting respiratory carbon loss. *The Plant Cell*, 31, 297–314.
- An, W., Liu, X., Leavitt, S.W., Xu, G., Zeng, X., Wang, W. et al. (2014) Relative humidity history on the Batang-Litang Plateau of western China since 1755 reconstructed from tree-ring  $\delta^{18}\text{O}$  and  $\delta\text{D}$ . *Climate Dynamics*, 42, 2639–2654.
- Augusti, A., Betson, T.R. & Schleucher, J. (2006) Hydrogen exchange during cellulose synthesis distinguishes climatic and biochemical isotope fractionations in tree rings. *New Phytologist*, 172, 490–499.
- Augusti, A., Betson, T.R. & Schleucher, J. (2008) Deriving correlated climate and physiological signals from deuterium isotopomers in tree rings. *Chemical Geology*, 252, 1–8.

- Baca Cabrera, J.C., Hirl, R.T., Schäufele, R., Zhu, J., Liu, H., Ogée, J. et al. (2021).  $^{18}\text{O}$  enrichment of leaf cellulose correlated with  $^{18}\text{O}$  enrichment of leaf sucrose but not bulk leaf water in a  $\text{C}_3$  grass across contrasts of atmospheric  $\text{CO}_2$  concentration and air humidity. <https://doi.org/10.21203/rs.3.rs-596094/v1>
- Barbour, M.M. (1999) *A physiological study of organic oxygen isotope composition*. Canberra: Australian National University.
- Barbour, M.M. & Farquhar, G.D. (2000) Relative humidity- and ABA-induced variation in carbon and oxygen isotope ratios of cotton leaves. *Plant, Cell & Environment*, 23, 473–485.
- Barbour, M.M., Fischer, R.A., Sayre, K.D. & Farquhar, G.D. (2000a) Oxygen isotope ratio of leaf and grain material correlates with stomatal conductance and grain yield in irrigated wheat. *Functional Plant Biology*, 27, 625–637.
- Barbour, M.M., Schurr, U., Henry, B.K., Wong, S.C. & Farquhar, G.D. (2000b) Variation in the oxygen isotope ratio of phloem sap sucrose from castor bean. Evidence in support of the Péclet effect. *Plant Physiology*, 123, 671–680.
- Barnard, R.L., de Bello, F., Gilgen, A.K. & Buchmann, N. (2006) The  $\delta^{18}\text{O}$  of root crown water best reflects source water  $\delta^{18}\text{O}$  in different types of herbaceous species. *Rapid Communications in Mass Spectrometry*, 20, 3799–3802.
- Byrn, M. & Calvin, M. (1966) Oxygen-18 exchange reactions of aldehydes and ketones. *Journal of the American Chemical Society*, 88, 1916–1922.
- Cernusak, L.A., Barbour, M.M., Arndt, S.K., Cheesman, A.W., English, N.B., Feild, T.S. et al. (2016) Stable isotopes in leaf water of terrestrial plants. *Plant, Cell & Environment*, 39, 1087–1102.
- Cernusak, L.A., Farquhar, G.D. & Pate, J.S. (2005) Environmental and physiological controls over oxygen and carbon isotope composition of Tasmanian blue gum, *Eucalyptus globulus*. *Tree Physiology*, 25, 129–146.
- Cernusak, L.A., Farquhar, G.D., Wong, S.C. & Stuart-Williams, H. (2004) Measurement and interpretation of the oxygen isotope composition of carbon dioxide respired by leaves in the dark. *Plant Physiology*, 136, 3350–3363.
- Cernusak, L.A., Pate, J.S. & Farquhar, G.D. (2002) Diurnal variation in the stable isotope composition of water and dry matter in fruiting *Lupinus angustifolius* under field conditions. *Plant, Cell & Environment*, 25, 893–907.
- Cernusak, L.A., Wong, S.-C. & Farquhar, G.D. (2003) Oxygen isotope composition of phloem sap in relation to leaf water in *Ricinus communis*. *Functional Plant Biology*, 30, 1059–1070.
- Cheesman, A.W. & Cernusak, L.A. (2016) Infidelity in the outback: climate signal recorded in  $\Delta 18\text{O}$  of leaf but not branch cellulose of eucalypts across an Australian aridity gradient. *Tree Physiology*, 37, 554–564.
- Chen, Y., Helliker, B.R., Tang, X., Li, F., Zhou, Y. & Song, X. (2020) Stem water cryogenic extraction biases estimation in deuterium isotope composition of plant source water. *Proceedings of the National Academy of Sciences of the United States of America*, 117, 33345–33350.
- Cormier, M.-A., Werner, R.A., Sauer, P.E., Gröcke, D.R., Leuenberger, M.C., Wieloch, T. et al. (2018)  $2\text{H}$ -fractionations during the biosynthesis of carbohydrates and lipids imprint a metabolic signal on the  $\delta^2\text{H}$  values of plant organic compounds. *New Phytologist*, 218, 479–491.
- Craig, H. & Gordon, L.I. (1965) Deuterium and oxygen-18 variations in the ocean and the marine atmosphere. In: Tongiorgi, E. (Ed.) *Proceedings of a Conference on Stable Isotopes in Oceanographic Studies and Palaeotemperatures*. Pisa: Lischi and Figli, pp. 9–130.
- Cueni, F., Nelson, D.B., Boner, M. & Kahmen, A. (2021) Using plant physiological stable oxygen isotope models to counter food fraud. *Scientific Reports*, 11, 17314.
- Dancer, J., Hatzfeld, W.-D. & Stitt, M. (1990) Cytosolic cycles regulate the turnover of sucrose in heterotrophic cell-suspension cultures of *Chenopodium rubrum* L. *Planta*, 182, 223–231.
- DeNiro, M.J. & Cooper, L.W. (1989) Post-photosynthetic modification of oxygen isotope ratios of carbohydrates in the potato: implications for paleoclimatic reconstruction based upon isotopic analysis of wood cellulose. *Geochimica et Cosmochimica Acta*, 53, 2573–2580.
- Ehlers, I., Augusti, A., Betson, T.R., Nilsson, M.B., Marshall, J.D. & Schleucher, J. (2015) Detecting long-term metabolic shifts using isotopomers:  $\text{CO}_2$ -driven suppression of photorespiration in  $\text{C}_3$  plants over the 20th century. *Proceedings of the National Academy of Sciences of the United States of America*, 112, 15585.
- Farquhar, G.D., Barbour, M.M. & Henry, B.K. (1998) Interpretation of oxygen isotope composition of leaf material. In: Griffiths, H. (Ed.) *Stable isotopes: integration of biological, ecological, and geochemical processes*. Oxford: BIOS Scientific Publishers Ltd. pp. 27–48.
- Farquhar, G.D. & Lloyd, J. (1993) Carbon and oxygen isotope effects in the exchange of carbon dioxide between terrestrial plants and the atmosphere. In: Ehleringer, J.R., Hall, A.E. & Farquhar, G.D. (Eds.) *Stable isotopes and plant carbon-water relations*. San Diego: Academic Press. pp. 47–70.
- Gaudinski, J.B., Dawson, T.E., Quideau, S., Schuur, E.A., Roden, J.S., Trumbore, S.E. et al. (2005) Comparative analysis of cellulose preparation techniques for use with  $^{13}\text{C}$ ,  $^{14}\text{C}$ , AND  $^{18}\text{O}$  isotopic measurements. *Analytical Chemistry*, 77, 7212–7224.
- Gessler, A., Brandes, E., Buchmann, N., Helle, G., Rennenberg, H. & Barnard, R. (2009) Tracing carbon and oxygen isotope signals from newly assimilated sugars in the leaves to the tree-ring archive. *Plant, Cell & Environment*, 32, 780–795.
- Gessler, A., Peuke, A.D., Keitel, C. & Farquhar, G.D. (2007) Oxygen isotope enrichment of organic matter in *Ricinus communis* during the diel course and as affected by assimilate transport. *New Phytologist*, 174, 600–613.
- Guerrieri, R., Belmecheri, S., Ollinger, S.V., Asbjornsen, H., Jennings, K., Xiao, J. et al. (2019) Disentangling the role of photosynthesis and stomatal conductance on rising forest water-use efficiency. *Proceedings of the National Academy of Sciences*, 116, 16909–16914.
- Hanson, K.R. & McHale, N.A. (1988) A starchless mutant of *Nicotiana glauca* containing a modified plastid phosphoglucomutase. *Plant Physiology*, 88, 838–844.
- Hatzfeld, W.-D. & Stitt, M. (1990) A study of the rate of recycling of triose phosphates in heterotrophic *Chenopodium rubrum* cells, potato tubers, and maize endosperm. *Planta*, 180, 198–204.
- Hayes, J.M. (2018) Fractionation of carbon and hydrogen isotopes in biosynthetic processes. In: Valley, J.W. & Cole, D.R. (Eds.) *Stable isotope geochemistry*. Washington, DC: De Gruyter, pp. 225–278.
- Helliker, B.R. & Richter, S.L. (2008) Subtropical to boreal convergence of tree-leaf temperatures. *Nature*, 454, 511–514.
- Hill, S.A., Waterhouse, J.S., Field, E.M., Switsur, V.R. & ap Rees, T. (1995) Rapid recycling of triose phosphates in oak stem tissue. *Plant, Cell & Environment*, 18, 931–936.
- Hirl, R.T., Ogée, J., Ostler, U., Schäufele, R., Baca Cabrera, J.C., Zhu, J. et al. (2021) Temperature-sensitive biochemical  $^{18}\text{O}$ -fractionation and humidity-dependent attenuation factor are needed to predict  $\delta^{18}\text{O}$  of cellulose from leaf water in a grassland ecosystem. *New Phytologist*, 229, 3156–3171.
- Huber, S.C. (1989) Biochemical mechanism for regulation of sucrose accumulation in leaves during photosynthesis. *Plant Physiology*, 91(2), 656–662. <https://doi.org/10.1104/pp.91.2.656>
- Ivakov, A., Flis, A., Apelt, F., Fünfgeld, M., Scherer, U., Stitt, M. et al. (2017) Cellulose synthesis and cell expansion are regulated by different mechanisms in growing Arabidopsis hypocotyls. *The Plant Cell*, 29, 1305–1315.
- Kahmen, A., Simonin, K., Tu, K.P., Merchant, A., Callister, A., Siegwolf, R. et al. (2008) Effects of environmental parameters, leaf physiological properties and leaf water relations on leaf water  $\delta^{18}\text{O}$  enrichment in different Eucalyptus species. *Plant, Cell & Environment*, 31, 738–751.

- Knowles, J.R. & Albery, W.J. (1977) Perfection in enzyme catalysis: the energetics of triosephosphate isomerase. *Accounts of Chemical Research*, 10, 105–111.
- Kölling, K., Thalmann, M., Müller, A., Jenny, C. & Zeeman, S.C. (2015) Carbon partitioning in *Arabidopsis thaliana* is a dynamic process controlled by the plants metabolic status and its circadian clock. *Plant, Cell & Environment*, 38, 1965–1979.
- Landhäusser, S.M., Chow, P.S., Dickman, L.T., Furze, M.E., Kuhlman, I., Schmid, S. et al. (2018) Standardized protocols and procedures can precisely and accurately quantify non-structural carbohydrates. *Tree Physiology*, 38, 1764–1778.
- Leadlay, P.F., Albery, W.J. & Knowles, J.R. (1976) Energetics of triosephosphate isomerase: deuterium isotope effects in the enzyme-catalyzed reaction. *Biochemistry*, 15, 5617–5620.
- Lehmann, M.M., Egli, M., Brinkmann, N., Werner, R.A., Saurer, M. & Kahmen, A. (2020) Improving the extraction and purification of leaf and phloem sugars for oxygen isotope analyses. *Rapid Communications in Mass Spectrometry*, 34, e8854.
- Lehmann, M.M., Gamarra, B., Kahmen, A., Siegwolf, R.T.W. & Saurer, M. (2017) Oxygen isotope fractionations across individual leaf carbohydrates in grass and tree species. *Plant, Cell & Environment*, 40, 1658–1670.
- Lehmann, M.M., Ghiasi, S., George, G.M., Cormier, M.-A., Gessler, A., Saurer, M. et al. (2019) Influence of starch deficiency on photosynthetic and post-photosynthetic carbon isotope fractionations. *Journal of Experimental Botany*, 70, 1829–1841.
- Lehmann, M.M., Goldsmith, G.R., Mirande-Ney, C., Weigt, R.B., Schönbeck, L., Kahmen, A. et al. (2020) The  $^{18}\text{O}$ -signal transfer from water vapour to leaf water and assimilates varies among plant species and growth forms. *Plant, Cell & Environment*, 43, 510–523.
- Lehmann, M.M., Vitali, V., Schuler, P., Leuenberger, M. & Saurer, M. (2021) More than climate: hydrogen isotope ratios in tree rings as novel plant physiological indicator for stress conditions. *Dendrochronologia*, 65, 125788.
- Libby, L.M., Pandolfi, L.J., Payton, P.H., Marshall, J., Becker, B. & Gierzt-Sienbenlist, V. (1976) Isotopic tree thermometers. *Nature*, 261, 284–288.
- Luo, Y.-H., Steinberg, L., Suda, S., Kumazawa, S., Mitsui, A. (1991). Extremely low D/H ratios of photoproducted hydrogen by Cyanobacteria. *Plant & Cell Physiology*. <https://doi.org/10.1093/oxfordjournals.pcp.a078158>
- Luo, Y.-H. & Sternberg, L. (1992) Hydrogen and oxygen isotopic fractionation during heterotrophic cellulose synthesis. *Journal of Experimental Botany*, 43, 47–50.
- Ma, R., Zhao, Y., Liu, L., Zhu, Z., Wang, B., Wang, Y. et al. (2020) Novel Position-specific  $^{18}\text{O}/^{16}\text{O}$  measurement of carbohydrates. II. The complete intramolecular  $^{18}\text{O}/^{16}\text{O}$  profile of the glucose unit in a starch of  $\text{C}_4$  origin. *Analytical Chemistry*, 92, 7462–7470.
- Nabeshima, E., Nakatsuka, T., Kagawa, A., Hiura, T. & Funada, R. (2018) Seasonal changes of  $\delta\text{D}$  and  $\delta^{18}\text{O}$  in tree-ring cellulose of *Quercus crispula* suggest a change in post-photosynthetic processes during earlywood growth. *Tree Physiology*, 38, 1829–1840.
- Newberry, S.L., Nelson, D.B. & Kahmen, A. (2017) Cryogenic vacuum artifacts do not affect plant water-uptake studies using stable isotope analysis. *Ecohydrology*, 10, e1892.
- O'Donoghue, A.C., Amyes, T.L. & Richard, J.P. (2005a) Hydron transfer catalyzed by triosephosphate isomerase. Products of isomerization of (R)-glyceraldehyde 3-phosphate in  $\text{D}_2\text{O}$ . *Biochemistry*, 44, 2610–2621.
- O'Donoghue, A.C., Amyes, T.L. & Richard, J.P. (2005b) Hydron transfer catalyzed by triosephosphate isomerase. Products of isomerization of dihydroxyacetone phosphate in  $\text{D}_2\text{O}$ . *Biochemistry*, 44, 2622–2631.
- R Core Team. (2019) *R: a language and environment for statistical computing*.
- Rieder, S.V. & Rose, I.A. (1959) The mechanism of the triosephosphate isomerase reaction. *Journal of Biological Chemistry*, 234, 1007–1010.
- Roden, J.S., Lin, G. & Ehleringer, J.R. (2000) A mechanistic model for interpretation of hydrogen and oxygen isotope ratios in tree-ring cellulose. *Geochimica et Cosmochimica Acta*, 64, 21–35.
- Rose, I.A. & O'Connell, E.L. (1961) Intramolecular hydrogen transfer in the phosphoglucose isomerase reaction. *Journal of Biological Chemistry*, 236, 3086–3092.
- Sanchez-Bragado, R., Serret, M.D., Marimon, R.M., Bort, J. & Araus, J.L. (2019) The hydrogen isotope composition  $\delta(2)\text{H}$  reflects plant performance. *Plant Physiology*, 180, 793–812.
- Sargeant, C.I., Singer, M.B. & Vallet-Coulomb, C. (2019) Identification of source-water oxygen isotopes in trees toolkit (ISO-tool) for deciphering historical water use by forest trees. *Water Resources Research*, 55, 10954–10975.
- Scheidegger, Y., Saurer, M., Bahn, M. & Siegwolf, R. (2000) Linking stable oxygen and carbon isotopes with stomatal conductance and photosynthetic capacity: a conceptual model. *Oecologia*, 125, 350–357.
- Schleucher, J., Vanderveer, P., Markley, J.L. & Sharkey, T.D. (1999) Intramolecular deuterium distributions reveal disequilibrium of chloroplast phosphoglucose isomerase. *Plant, Cell & Environment*, 22, 525–533.
- Schmidt, H.-L., Werner, R.A. & Eisenreich, W. (2003) Systematics of  $2\text{H}$  patterns in natural compounds and its importance for the elucidation of biosynthetic pathways. *Phytochemistry Reviews*, 2, 61–85.
- Schmidt, H.L., Werner, R.A. & Rossmann, A. (2001)  $^{18}\text{O}$  pattern and biosynthesis of natural plant products. *Phytochemistry*, 58, 9–32.
- Schuler, P., Cormier, M.A., Werner, R.A., Buchmann, N., Gessler, A., Vitali, V., Saurer, M., Lehmann, M.M. (2021) A high-temperature water vapor equilibration method to determine non-exchangeable hydrogen isotope ratios of sugar, starch and cellulose. *Plant, Cell & Environment*, 45, 12–22.
- Song, X., Farquhar, G.D., Gessler, A. & Barbour, M.M. (2014) Turnover time of the non-structural carbohydrate pool influences  $\delta^{18}\text{O}$  of leaf cellulose. *Plant, Cell & Environment*, 37, 2500–2507.
- Sternberg, L. & DeNiro, M.J.D. (1983) Biogeochemical implications of the isotopic equilibrium fractionation factor between the oxygen atoms of acetone and water. *Geochimica et Cosmochimica Acta*, 47, 2271–2274.
- Sternberg, L. & Ellsworth, P.F.V. (2011) Divergent biochemical fractionation, not convergent temperature, explains cellulose oxygen isotope enrichment across latitudes. *PLoS One*, 6, e28040.
- Stitt, M. & Zeeman, S.C. (2012) Starch turnover: pathways, regulation and role in growth. *Current Opinion in Plant Biology*, 15, 282–292.
- Sulpice, R., Flis, A., Ivakov, A.A., Apelt, F., Krohn, N., Encke, B. et al. (2014) *Arabidopsis* coordinates the diurnal regulation of carbon allocation and growth across a wide range of photoperiods. *Molecular Plant*, 7, 137–155.
- Sulpice, R., Pyl, E.-T., Ishihara, H., Trenkamp, S., Steinfath, M., Witucka-Wall, H. et al. (2009) Starch as a major integrator in the regulation of plant growth. *Proceedings of the National Academy of Sciences of the United States of America*, 106, 10348–10353.
- Szejner, P., Clute, T., Anderson, E., Evans, M.N. & Hu, J. (2020) Reduction in lumen area is associated with the  $\delta^{18}\text{O}$  exchange between sugars and source water during cellulose synthesis. *New Phytologist*, 226, 1583–1593.
- Tcherkez, G. (2010) *Isotopie biologique—introduction aux effets isotopiques et à leurs applications en biologie*. Éditions Tec et Doc.
- Voelker, S.L., Brooks, J.R., Meinzer, F.C., Roden, J., Pazdur, A., Pawelczyk, S. et al. (2014) Reconstructing relative humidity from plant  $\delta^{18}\text{O}$  and  $\delta\text{D}$  as deuterium deviations from the global meteoric water line. *Ecological Applications*, 24, 960–975.
- Warton, D.I., Duursma, R.A., Falster, D.S. & Taskinen, S. (2012) smatr 3—an R package for estimation and inference about allometric lines. *Methods in Ecology and Evolution*, 3, 257–259.

- Waterhouse, J.S., Switsur, V.R., Barker, A.C., Carter, A.H.C. & Robertson, I. (2002) Oxygen and hydrogen isotope ratios in tree rings: how well do models predict observed values? *Earth and Planetary Science Letters*, 201, 421–430.
- Weise, S.E., Weber, A.P.M., & Sharkey, T.D. (2004). Maltose is the major form of carbon exported from the chloroplast at night. *Planta*, 218(3), 474–482. <https://doi.org/10.1007/s00425-003-1128-y>
- Wieloch, T., Augusti, A. & Schleucher, J. (2022a) Anaplerotic flux into the Calvin–Benson cycle: hydrogen isotope evidence for in vivo occurrence in C<sub>3</sub> metabolism. *New Phytologist*, 234, 405–461.
- Wieloch, T., Grabner, M., Augusti, A., Serk, H., Ehlers, I., Yu, J. et al. (2022b) Metabolism is a major driver of hydrogen isotope fractionation recorded in tree-ring glucose of *Pinus nigra*. *New Phytologist*, 234, 449–461.
- Wijker, R.S., Sessions, A.L., Fuhrer, T. & Phan, M. (2019) <sup>2</sup>H/<sup>1</sup>H variation in microbial lipids is controlled by NADPH metabolism. *Proceedings of the National Academy of Sciences of the United States of America*, 116, 12173–12182.
- Yakir, D. & DeNiro, M.J. (1990) Oxygen and hydrogen isotope fractionation during cellulose metabolism in *Lemna gibba* L. *Plant Physiology*, 93, 325–332.
- Zhou, Y., Zhang, B., Stuart-Williams, H., Grice, K., Hocart, C.H., Gessler, A. et al. (2018) On the contributions of photorespiration and

- compartmentation to the contrasting intramolecular <sup>2</sup>H profiles of C<sub>3</sub> and C<sub>4</sub> plant sugars. *Phytochemistry*, 145, 197–206.
- Zhu, Z., Yin, X., Song, X., Wang, B., Ma, R., Zhao, Y. et al. (2020) Leaf transition from heterotrophy to autotrophy is recorded in the intraleaf C, H and O isotope patterns of leaf organic matter. *Rapid Communications in Mass Spectrometry*, 34, e8840.

#### SUPPORTING INFORMATION

Additional supporting information can be found online in the Supporting Information section at the end of this article.

**How to cite this article:** Holloway-Phillips, M., Baan, J., Nelson, D.B., Lehmann, M.M., Tcherkez, G. & Kahmen, A. (2022) Species variation in the hydrogen isotope composition of leaf cellulose is mostly driven by isotopic variation in leaf sucrose. *Plant, Cell & Environment*, 1–16. <https://doi.org/10.1111/pce.14362>